AGU PUBLICATIONS

JGR

Journal of Geophysical Research: Atmospheres

RESEARCH ARTICLE
10.1002/2017JD027917

Key Points:
- Elevated CO_2 correlates with enhancements in several National Ambient Air Quality Standard criteria pollutants
- CO_2 provides insight into meteorological, chemical, and transport processes during persistent cold air pool events
- Emission inventories overestimate $CO:CO_2$ and $NO_x:CO_2$ ratios

Correspondence to:
R. Bares,
ryan.bares@utah.edu

Citation:
Bares, R., Lin, J. C., Hoch, S. W., Baasandorj, M., Mendoza, D. L., Fasoli, B., et al. (2018). The wintertime covariation of CO_2 and criteria pollutants in an urban valley of the western United States. *Journal of Geophysical Research: Atmospheres*, *123*, 2684–2703. https://doi.org/10.1002/2017JD027917

Received 18 OCT 2017
Accepted 18 FEB 2018
Accepted article online 23 FEB 2018
Published online 12 MAR 2018
Corrected 3 AUG 2018

This article was corrected on 3 AUG 2018. See the end of the full text for details.

The Wintertime Covariation of CO_2 and Criteria Pollutants in an Urban Valley of the Western United States

Ryan Bares[1,2], John C. Lin[1,2], Sebastian W. Hoch[1], Munkhbayar Baasandorj[1,3], Daniel L. Mendoza[1], Ben Fasoli[1,2], Logan Mitchell[1], Douglas Catharine[1,2], and Britton B. Stephens[4]

[1]Department Atmospheric Sciences, University of Utah, Salt Lake City, UT, USA, [2]Utah Atmospheric Trace Gas and Air Quality Lab, University of Utah, Salt Lake City, UT, USA, [3]Division of Air Quality, Utah Department of Environmental Quality, Salt Lake City, UT, USA, [4]National Center for Atmospheric Research, Boulder, CO, USA

Abstract Numerous mountain valleys experience wintertime particulate pollution events, when persistent cold air pools (PCAPs) develop and inhibit atmospheric mixing, leading to the accumulation of pollutants. Here we examine the relationships between trace gases and criteria pollutants during winter in Utah's Salt Lake Valley, in an effort to better understand the roles of transport versus chemical processes during differing meteorological conditions as well as insights into how targeted reductions in greenhouse gases will impact local air quality in varying meteorological conditions. CO_2 is a chemically inert gas that is coemitted during fossil fuel combustion with pollutants. Many of these coemitted pollutants are precursors that react chemically to form secondary particulate matter. Thus, CO_2 can serve as a stable tracer and potentially help distinguish transport versus chemical influences on pollutants. During the winter of 2015–2016, we isolated enhancements in CO_2 over baseline levels due to urban emissions ("CO_{2ex}"). CO_{2ex} was paired with similar excesses in other pollutant concentrations. These relationships were examined during different wintertime conditions and stages of pollution episodes: (a) Non-PCAP, (b) beginning, and (c) latter stages of an episode. We found that CO_{2ex} is a good indicator of the presence of gaseous criteria pollutants and a reasonable indicator of $PM_{2.5}$. Additionally, the relationships between CO_{2ex} and criteria pollutants differ during different phases of PCAP events which provide insight into meteorological and transport processes. Lastly, we found a slight overestimation of $CO:CO_2$ emission ratios and a considerable overestimation of $NO_x:CO_2$ by existing inventories for the Salt Lake Valley.

1. Introduction

Numerous topographic basins in the Intermountain West region of the United States, and worldwide, experience wintertime persistent cold air pool (PCAP) episodes (Gillies et al., 2010; Gorski et al., 2015; Green et al., 2015; Kondo et al., 1989; Malek et al., 2006; Panday et al., 2009; Villalobos-Pietrini et al., 2006). PCAP events are multiday episodes of high atmospheric stability associated with synoptic scale high-pressure ridges, coinciding with reduced surface temperatures and insolation due to high surface albedo from snow cover (Lareau et al., 2013; Silcox et al., 2012; Whiteman et al., 2014). Under such conditions, vertical mixing is suppressed, enabling accumulation of pollutants such as nitrogen oxides (NO_x = NO+NO_2), carbon monoxide (CO), and fine particulate matter ($PM_{2.5}$) within the shallow boundary layer, with $PM_{2.5}$ levels exceeding the National Ambient Air Quality Standards (NAAQS) of 35 $\mu g/m^3$ (Baasandorj et al., 2017; Long et al., 2003; Malek et al., 2006; Silva et al., 2007; Whiteman et al., 2010, 2014). The main constituent of $PM_{2.5}$ is secondary ammonium nitrate (NH_4NO_3), which accounts for 70–80% of the total mass (Baasandorj et al., 2017; Kelly et al., 2013; Kuprov et al., 2014; SIP, 2014), which forms in the atmosphere through a reversible reaction of ammonia (NH_3) and nitric acid (HNO_3) (Stelson & Seinfeld, 1982). While NH_3 is emitted directly into the atmosphere predominantly from agricultural sources (Behera et al., 2013), nitric acid is formed in the atmosphere via NO_x reaction with OH during the day and through the nighttime chemistry that involves the heterogeneous reactions of N_2O_5 (Brown & Stutz, 2012).

Long-lived pollution episodes in Utah's Salt Lake Valley (SLV) often exhibit a distinct pattern, with (1) an initial Buildup phase, during which $PM_{2.5}$ concentrations increase at a rate of ~6 to 10 $\mu g/m^3$ per day, (2) a later period with plateauing $PM_{2.5}$ concentrations, and (3) the clean-out phase associated with the breakup of a PCAP (Baasandorj et al., 2017; Whiteman et al., 2014). Baasandorj et al. (2017) discussed the evolution of chemical

composition during the different stages and underscored the importance of the interaction between the chemistry in the upper part of a PCAP and transport processes contributing to the surface $PM_{2.5}$ enhancements during the pollution episodes.

In this study, we examine the relationships in the SLV between NAAQS pollutants and CO_2, as well as describe the associated meteorological conditions during and outside of PCAP conditions during the winter of 2015–2016. By examining these relationships, we can understand transport and chemical processes during differing meteorological conditions as well as provide insight into how targeted reductions in greenhouse gases could impact local air quality. A week-long episode during this winter served as a case study. CO_2 is a long-lived, chemically stable species coemitted with other pollutants during fossil fuel combustion, including CO, NO, NO_2, and primary $PM_{2.5}$ (Kolb et al., 2002; Wallington et al., 2008; Watson et al., 1990). The importance of CO_2 as the dominant greenhouse gas responsible for anthropogenic climate forcing has resulted in the development of well-established measurement surface and aircraft networks around the world (Andrews et al., 2014; Tanset al., 1996; Turnbull et al., 2012; Turnbull, Karion, et al., 2011), which recently have been enhanced to include satellite sensors with global coverage (Butz et al., 2011; Crisp et al., 2012; Silva et al., 2013; Yokota et al., 2009).

There has been growing interest in measuring CO_2 in urban areas to understand the processes controlling carbon emissions, since cities are responsible for ~70% of anthropogenic CO_2 emissions globally (IEA, 2015). Cities around the world where intensive CO_2 observations and associated research efforts are taking place are Salt Lake City (McKain et al., 2012; Mitchell et al., 2018; Pataki et al., 2005), Paris (Dolman et al., 2006; Sarrat et al., 2007; Staufer et al., 2016), Osaka (Ueyama & Ando, 2016), Indianapolis (Lauvaux et al., 2016; Turnbull et al., 2015), Los Angeles (Newman et al., 2008; Newman et al., 2016), Rotterdam (Super et al., 2017), among others (Duren & Miller, 2012). If relationships between CO_2 concentrations and air pollutants in cities can be better understood, synergies between the growing effort to observe urban CO_2 and air quality can be realized. For instance, criteria pollutants can serve as additional tracers to help attribute variations in CO_2 to anthropogenic activities. One example is the use of CO:CO_2 ratios indicating the presence of fossil fuel combustion (Palmer et al., 2006; Turnbull et al., 2015; Turnbull, Karion, et al., 2011; Vardag et al., 2015). Conversely, CO_2 and other greenhouse gas measurements can be used to constrain emissions of criteria pollutants, as well as to quantify exposure to air pollution (Ahmadov et al., 2015; Wilkey et al., 2016).

In this paper, we make use of the Utah Urban Carbon Dioxide Network (UUCON) at the University of Utah (UOU). The UUCON network (consisting of eight sites) is located along the Wasatch Mountains of northern Utah, where over 80% of Utah's population is found. Among the eight UUCON sites, six are distributed throughout the greater Salt Lake City area (Figure 1), within the SLV, and several additional sites in surrounding valleys, with measurement locations in an array of land use types (Table 1). UUCON measurements began in 2001 (Pataki et al., 2003), offering one of the longest continuous urban multisite CO_2 records available (Mitchell et al., 2018), which provides an unprecedented opportunity to explore relationships between CO_2 and other pollutants.

In this paper, we first present the long-term relationship between CO_2 and $PM_{2.5}$ from 2003 to 2013. We then examine this relationship as well as the relationships between CO_2 and other pollutants (CH_4, NO_x, and CO) in detail during an intensive measurement campaign in December 2015 to February 2016, as part of the Salt Lake Valley Wintertime $PM_{2.5}$ Study (Baasandorj et al., 2017).

We seek to make use of the unique stable atmospheric conditions during PCAP events, in which the atmosphere over the SLV serves as a "smog chamber" in order to probe the CO_2-pollutant relationships and the meteorological conditions that drive them. This work builds upon a previous paper by Pataki et al. (2005), in which SLV CO_2 observations were used to establish the use of CO_2 as an inert tracer of atmospheric transport, as well as the study by Gorski et al. (2015), which used CO_2 as an indicator for anthropogenic combustion in relation to distinct isotopic signatures of urban water vapor during PCAP conditions. This work expands beyond the Pataki et al. (2005) and Gorski et al. (2015) analyses in several key ways: (1) a significantly larger suite of pollutant observations colocated with CO_2 that were collected for a longer period of time; (2) addition of a new CO_2 site ("Suncrest") at higher elevation; (3) availability of enhanced meteorological observations; and (4) comparisons against emission inventories.

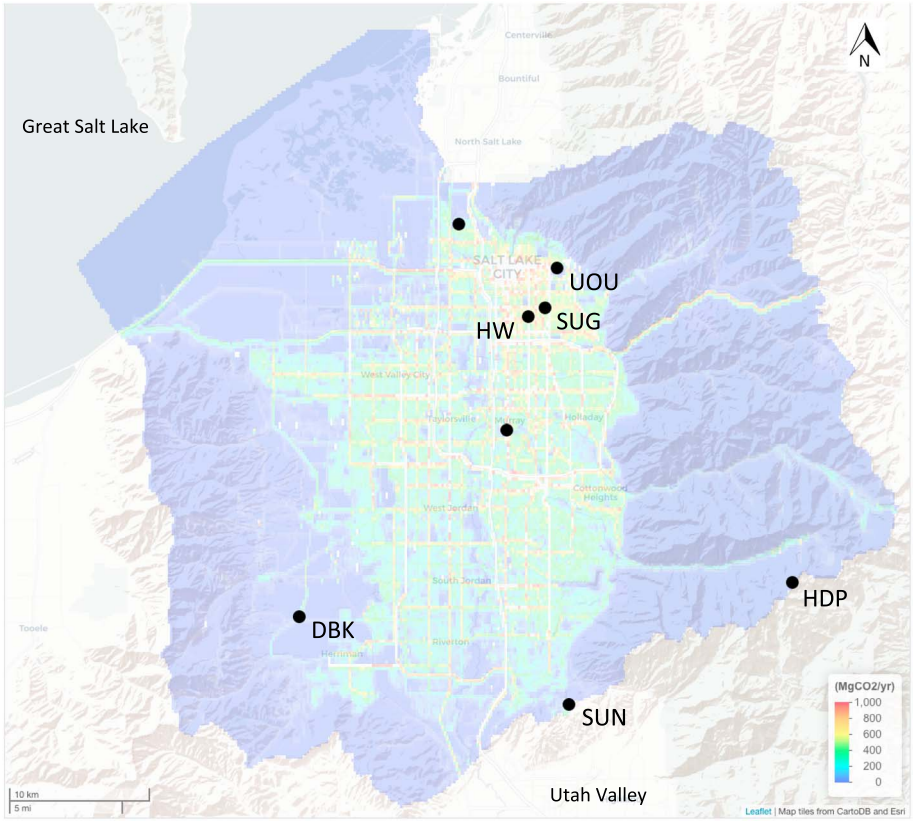

Figure 1. Map of the Salt Lake Valley. Black dots indicate measurement sites. Dots without three-letter site codes indicate measurement locations not utilized in this analysis. Color scale shows Hestia inventory-derived county-wide emissions aggregated by sector in megagrams of CO_2 per year per grid cell at 0.002° × 0.002° grid spacing.

The key questions addressed in this study are the following:

1. Is the presence of elevated CO_2 a good proxy for the enhancements in criteria pollutants (CO, NO_x, and $PM_{2.5}$)?
2. Are the relationships between CO_2 and criteria pollutants different during different phases of a PCAP?
3. How do the observed CO:CO_2 and NO_x:CO_2 ratios compare to existing literature and inventory estimates?

2. Methods

2.1. Site Locations and Measurement Methods

The Utah Atmospheric Trace Gas and Air Quality (U-ATAQ) lab is located on the top floor of the eight-story William Browning Building on the UOU campus, which is situated on the northeastern bench of the SLV (Figure 1). The instrument inlets are located on the roof of the building, 33 m above ground level. CO_2, CO, CH_4, NO, NO_2, and $PM_{2.5}$ were measured at the U-ATAQ lab between December 2015 and February 2016 as part of the Salt Lake Valley Wintertime $PM_{2.5}$ Study (Baasandorj et al., 2017). In addition, a variety of

Table 1
Measurement Locations in the Salt Lake Valley

Site code	Site name	Latitude	Longitude	Elevation (m above sea level)	Inlet height (m above ground level)	Species measured	Land use
UOU	University of Utah	40.763	111.848	1,430	31.5	CO_2, CH_4, NO_x, CO, $PM_{2.5}$	Mixed residential commercial
DBK	Daybreak	40.538	112.070	1,580	5.05	CO_2	Rural sagebrush steppe
SUG	Sugarhouse	40.740	111.858	1,339	3.86	CO_2	Residential
SUN	Suncrest	40.480	111.836	1,859	4.22	CO_2	Midaltitude, residential
HDP	Hidden Peak	40.560	111.650	3,351	17.1	CO_2	High elevation/background

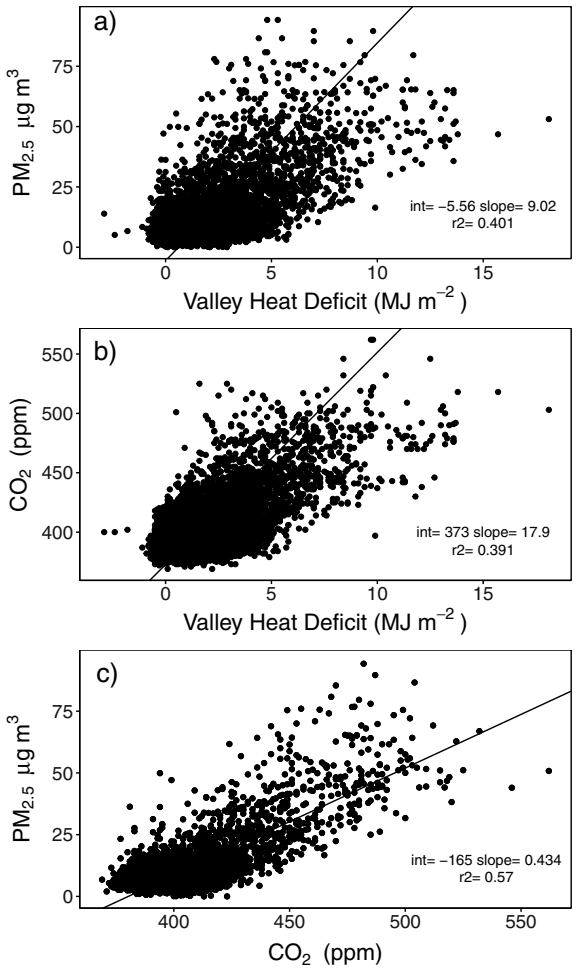

Figure 2. Linear regressions derived from the long-term data set spanning from 2003 to 2013. (a) Relationship between $PM_{2.5}$ in micrograms per cubic meter and valley heat deficit in megajoules per square meter. (b) The relationship between CO_2 mixing ratio and valley heat deficit. (c) The relationship between $PM_{2.5}$ and CO_2.

meteorological observations were conducted by MesoWest (Horel et al., 2002). The William Browning Building is heated by high-temperature water provided from a heating plant located ~1 km away, resulting in an absence of on-site combustion for heating. Other potential sources of contamination (e.g., fume hoods and vents) at the UOU site and all other sites used in this analysis have been examined, and inlet locations were selected in an effort to mitigate any potential source contamination of the measurements.

CO_2 and CH_4 measurements were made using a Los Gatos Research Ultra Portable Greenhouse Gas Spectrometer (Model 907-0011, Los Gatos Research Inc., San Jose, CA). Calibration gases were introduced to the analyzer every 3 h using three whole-air, high-pressure reference gas cylinders with known CO_2 and CH_4 concentrations (tertiary to World Meteorological Organization X2007 CO_2 mole fraction scale, Zhao & Tans, 2006, and the NOAA04 CH_4 mole fraction scale, Dlugokencky et al., 2005). Concentrations of the calibration gases spanned the expected range of atmospheric concentrations. Measurements were recorded at 10 s frequency. All data used in this analysis were averaged from their native measurement frequency into hourly averages. Details regarding the calibration materials, measurement uncertainty, and post-processing for all CO_2 and CH_4 observations used in this analysis can be found in Gorski et al. (2015) and Foster et al. (2017), respectively.

CO, NO, NO_2, and NO_x observations were collected using Teledyne Advanced Pollution Instrumentation's gas filter correlation CO analyzer (Model 300 E) and NO_x analyzer (Model T200 U), respectively. $PM_{2.5}$ mass was measured using an 8500 filter dynamics measurement system (FDMS)—TEOM 1400ab ambient particulate monitor. Details regarding CO, NO_x, and $PM_{2.5}$ measurement protocols, uncertainty, and calibrations can be found in Baasandorj et al. (2017).

CO_2 observations from four other sites were used in this analysis (Figure 1 and Table 1): Suncrest (SUN), Daybreak (DBK), Sugarhouse (SUG), and Hidden Peak (HDP). SUN is located in a low-population density neighborhood which is situated in a midaltitude (1,858 m above sea level) location, 500 m above the valley floor but ~1,500 m below the tops of the nearby mountain tops (Figure 1). The unique elevation of SUN positions it outside the nocturnal boundary layer during PCAP conditions but within the well-mixed convective boundary layer (CBL) during the day as will be discussed below. Additionally, SUN and UOU are in close proximity to the nearby Wasatch Mountains and several tributary canyons, allowing for the presence of katabatic winds to inject free tropospheric clean air at these locations.

DBK is one of the longest-running sites within the UUCON network, located in a rural portion of SLV's southwestern corner (Figure 1 and Table 1). While this site generally represents the rural portion of the SLV (Pataki et al., 2003; Pataki et al., 2005), this region of the valley has seen the greatest rate of population increase and urban sprawl in recent years (Mitchell et al., 2018). Due to its elevation and remote location, DBK serves both as a rural CO_2 monitoring site during most times as well as an indicator of the spread of the urban plume during PCAP events, as noted in Pataki et al. (2005).

SUG is located on a residence in a dense residential neighborhood on the valley floor, near Hawthorne Elementary (HW) (Figure 1 and Table 1) and is located ~1 km east and 20 m higher in elevation from the Utah Division of Air Quality's flagship measurement site for the SLV, Hawthorne Elementary (Figure 1).

HDP is located at 3,351 m above sea level at the top of the Snowbird Ski Resort (Figure 1) and has been running since 2006 as part of the National Center for Atmospheric Research's Regional Atmospheric Continuous CO_2 Network in the Rocky Mountains (Stephens et al., 2011).

2.2. Long-Term Record

The long-term record used in this study has been described in detail by Whiteman et al. (2014) and contains twice daily valley heat deficits (see section 2.4), 24 h average CO_2 concentrations measured at UOU as part of the UUCON network, and $PM_{2.5}$ concentrations from various locations throughout the SLV between 2003 and 2013 (Figure 2).

2.3. Baseline Concentrations and Biological Fluxes

To isolate the enhancements in concentrations from urban emissions within the SLV, it is necessary to establish "baseline" conditions. We derived baseline concentrations using the lowest first percentile within a 24 h window centered around each hourly averaged data point, then applied a 24 h running average. This was done for all atmospheric constituents measured at each site; thus, the baseline is specific to individual locations (Figure 1 and Table 1) and covers all measured species. This baseline was then subtracted from the hourly averaged concentration to determine the excess concentrations (i.e., "CO_{2ex}") due to urban emissions of each species (Figure 3).

The 24 h window was chosen to study the day-to-day enhancements at subdaily time scales in an effort to isolate signatures of recent emissions. In this way, the baseline we selected is somewhat different from the concept of a "background" concentration, which remains unaffected by urban emissions. To contrast our baseline against a traditional concept of a background, we compared the baseline against regional background values based on a smoothing of observed CO_2 values at the HDP high elevation mountaintop site (Figure 1), as described in Mitchell et al. (2018).

We found a high degree of agreement between the baseline and regional background outside of PCAPs but a decoupling of the two methods during PCAP events (Figure 3). During PCAP events, the baseline tracked the CO_2 buildup, by design. This is especially noticeable during the long PCAP event in the first half of February 2016. In contrast, the HDP-derived background remained unchanged, hovering near 405 ppm with variations of less than 1 ppm over the study period. Thus, selecting a regional background site like HDP essentially applies a constant offset to the resulting excess concentrations and provides little to no additional information than when comparing mass or mole fraction concentrations. Linear regression analysis of baseline CO_2 compared to the baseline of other species (Table 2) identify very high degrees of correlation with r^2 values ranging from 0.89 to 0.94, indicating that the baseline values track the buildup of pollutants during PCAP conditions and during cleaner periods.

An added benefit to our baseline approach is that it is geographically specific for each site. Geographically specific phenomena are expected to be more relevant during PCAP events, when the lack of turbulent mixing leads to more pronounced spatial gradients between sites (Mitchell et al., 2018; Silcox et al., 2012). Additionally, many background sites are limited to observations of a single species (i.e., CO_2), while the baseline approach used in this analysis can be applied to each constituent of interest.

In addition to establishing the baseline, when examining excess CO_2 it is critical to understand how much local biological activity contributes as sources, through processes of respiration and decomposition, and as a sink through photosynthetic uptake. Previous research conducted in the SLV has identified minimal to negligible biological fluxes during the wintertime (Pataki et al., 2003; Pataki et al., 2005; Pataki et al., 2006; Pataki et al., 2007; Strong et al., 2011), especially relative to anthropogenic contributions.

2.4. Valley Heat Deficit and PCAP Conditions

Radiosonde observations launched twice daily from the Salt Lake International Airport are used to calculate the valley heat deficit (VHD), a quantitative, thermodynamic measure of atmospheric stability (Whiteman et al., 2014). The VHD represents the amount of heat needed to bring an atmospheric column with a specified height to a dry adiabatic lapse rate. Using VHD calculations based on the average valley depth of 2,200 m, Whiteman et al. (2014) found that when a VHD threshold of 4.04 MJ m^{-2} was exceeded, wintertime $PM_{2.5}$ concentrations begin to rise steadily. PCAP events can thus be defined as any event with at least three consecutive 12-hourly soundings yielding heat deficits greater than 4.04 MJ m^{-2}. Five events met these criteria during the study, as indicated by gray shaded areas on Figure 3, with one PCAP excluded at the beginning of the study due to the lack of reliable $PM_{2.5}$ data.

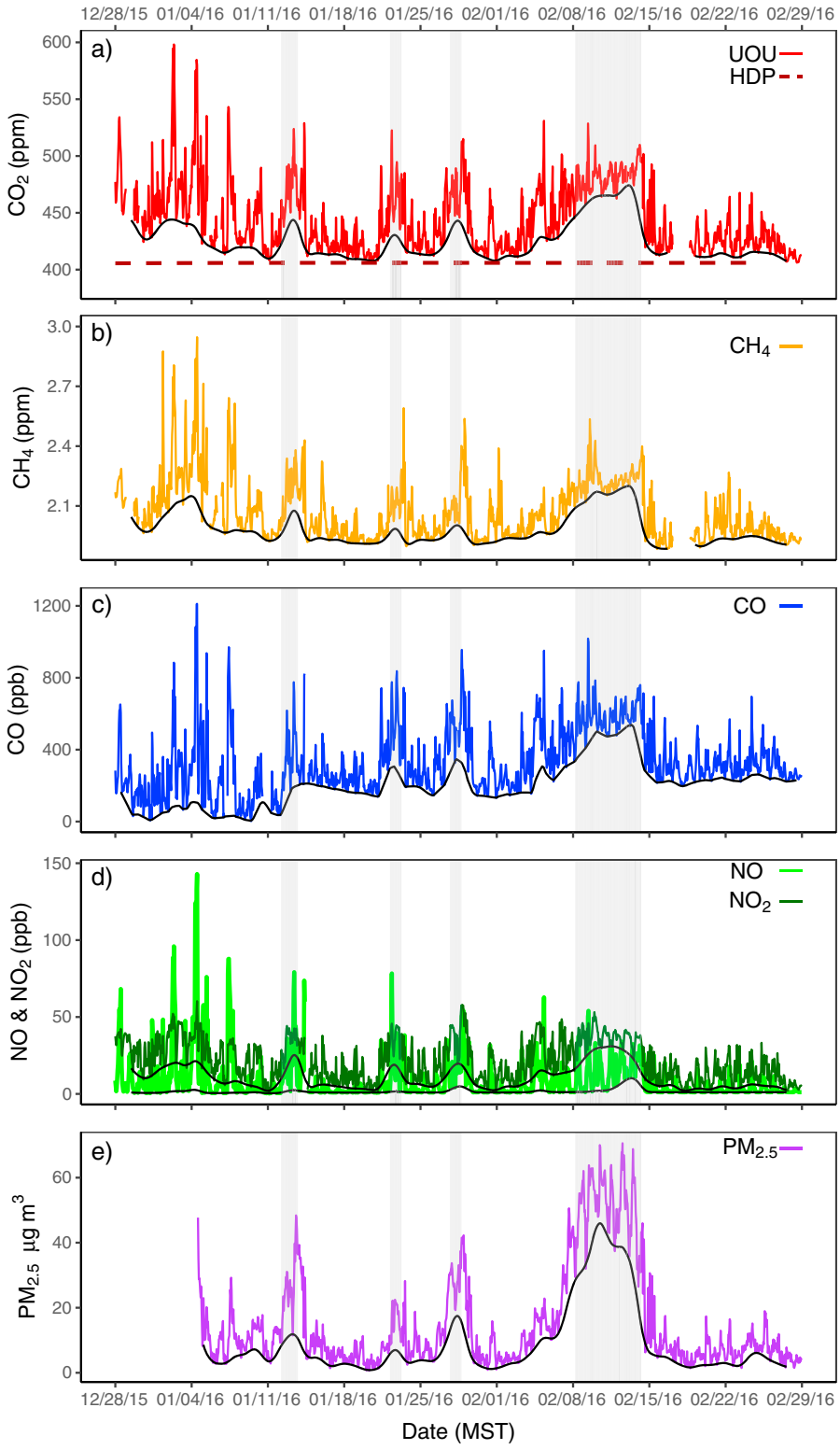

Figure 3. Time series of entire study period of (a) CO_2 mixing ratio from University of Utah (UOU) and Hidden Peak (HDP), with UOU observations of (b) CH_4 mixing ratio, (c) CO mixing ratio, (d) mixing ratios of NO and NO_2, and (e) $PM_{2.5}$ mass concentration. In all panels black line indicates calculated baseline concentrations from which excess concentrations are calculated. Gray shaded regions indicate persistent cold air pool conditions. This figure illustrates the intermittent periods of persistent cold air pools during a typical winter in the Salt Lake Valley.

Table 2
Slope, Standard Deviation and Correlation Coefficient for Each of the Linear Regressions in Figure 4

Relationship	Period	Slope	$\pm1\sigma$	r^2
CO_{ex}:CO_{2ex} (ppb:ppm)	Full sample period	7.38	0.165	0.79
	Non-PCAP	7.19	0.153	0.81
	PCAP	8.87	0.172	0.70
	Buildup	9.37	0.170	0.62
	Plateau	7.31	0.107	0.71
	Baseline	5.96[a]	0.040[a]	0.90[a]
NO_{xex}:CO_{2ex} (ppb:ppm)	Full sample period	0.91	0.020	0.90
	Non-PCAP	0.90	0.020	0.91
	PCAP	1.01	0.015	0.84
	Buildup	0.88	0.018	0.76
	Plateau	0.72	0.007	0.88
	Baseline	0.63	0.005	0.94
$PM_{2.5}$:CO_2 ($\mu g/m^3$:ppm)	Full sample period	0.49	0.019	0.56
	Long term	0.43	0.008	0.57
	Non-PCAP	0.28	0.016	0.47
	PCAP	0.95	0.060	0.11
	Buildup	0.68	0.026	0.29
	Plateau	−1.13	0.072	0.10
$PM_{2.5ex}$:CO_{2ex} ($\mu g/m^3$:ppm)	Full sample period	0.18	0.015	0.17
	Non-PCAP	0.17	0.014	0.28
	PCAP	0.00	0.014	0.00
	Buildup	0.00	0.015	0.00
	Plateau	0.10	0.018	0.01
	Baseline	0.64	0.009	0.92
CH_{4ex}:CO_{2ex} (ppb:ppm)	Full sample period	4.000	0.125	0.67
	Non-PCAP	4.447	0.127	0.70
	PCAP	3.000	0.102	0.46
	Buildup	2.197	0.111	0.23
	Plateau	3.593	0.070	0.77
	Baseline	4.312	0.133	0.89
$PM_{2.5ex}$:CH_{4ex} ($\mu g/m^3$:ppm)	Full sample period	162.00	12.442	0.20
	Non-PCAP	101.00	6.310	0.30
	PCAP	430.00	41.562	0.06
	Buildup	346.09	24.942	0.10
	Plateau	691.70	47.885	0.05
	Baseline	153.00	1.813	0.89

Note. Relationships from Figure 2c also reported. PCAP = persistent cold air pool.
[a]Excluded first 400 observations to account for zero offset.

In this study we are interested in the relationships between pollutants and CO_2 during PCAP periods, "Non-PCAP" conditions, and the "Buildup" and "Plateau" stages of a PCAP as identified by Baasandorj et al. (2017). Of the five PCAP events only one was long lived enough to exhibit the Buildup and Plateau stages and will be examined in detail in section 3.4.

2.5. Linear Regressions

To summarize relationships between excess concentrations of greenhouse gases (CO_2 and CH_4) and criteria pollutants, linear regression analysis was carried out on all species to extract the values of the slopes. All linear regressions were performed using model II major axis regression in the R statistical analysis software which reduces variance in both the *X* and *Y* axes, as described by Legendre and Legendre (1998) and Sokal and Rohlf (1995). Intercept offsets were allowed; thus, slopes were not fit to 0. Uncertainties for the slopes were calculated by bootstrapping 1,000 permutations of the data derived from randomly sampling the excess concentrations with replacement equal in size to the original data. Standard deviation of the slopes derived from the 1,000 regressions is reported.

2.6. Emission Inventories

County-wide emission estimates were provided as a base from the National Emissions Inventory (NEI) (National Emission Inventory, 2014; Pouliot et al., 2014) for the criteria pollutants (CO, NO_x, and $PM_{2.5}$), and the Vulcan data product (Gurney et al., 2009) for CO_2 emissions. Both of these data sets were scaled to 2015–2016 using fuel sale information from the Energy Information Administration (State Energy Data System, 2016), with 2002 and 2014 as the base years for Vulcan and NEI, respectively. The NEI is based primarily on data provided by state, local, and tribal air agencies for sources in their jurisdiction, released every 3 years, and supplemented with data from the U.S. Environmental Protection Agency. The Hestia CO_2 emissions product for Salt Lake City (Patarasuk et al., 2016) accounts for direct on-site CO_2 emissions from all anthropogenic sectors: that is, on-road, residential, commercial, industrial point, electricity generation, mobile off-road, airport, railroad, and commercial points.

County emission totals were spatially disaggregated using local data from the department of transportation and federal highway administration, parcel data from the tax assessor data, and population growth and construction activity data. Each sector's emissions were computed independently using temporal traffic profiles, building activity data, and point source activity data from the NEI and aggregated to produce a total hourly emissions flux for CO_2, CO, and NO_x (90% NO and 10% NO_2).

2.7. Diurnal Cycles and Meteorological Variables

Diurnal cycles were calculated by binning hourly averaged data by hour of day, then averaging each bin resulting in 24 observations for each cycle examined. Wind vectors were calculated for each hour of day using the vector components (*U* and *V*) from the above diurnal cycle calculations.

3. Results and Discussion

3.1. Long-Term Observations

Figure 2 shows the relationships between $PM_{2.5}$, CO_2, and VHD from 2003 to 2013. Note that no baseline was subtracted to derive the "excess" values. Thus, the relationships are different than the excess concentration

relationships explored below in section 3.2. Also, this relationship includes seasons well beyond the wintertime season explored elsewhere in this study; thus, primary particulate matter contributes significantly to this relationship, while secondary $PM_{2.5}$ drives the relationships during PCAP conditions. A statistically significant correlation was found between $PM_{2.5}$ and VHD (Figure 2a), in accordance with Whiteman et al. (2014), as well as between CO_2 and VHD. An even stronger correlation between CO_2 and $PM_{2.5}$ was observed, with $r^2 = 0.57$ (Figures 2b and 2c and Table 2).

3.2. Relationships and Enhancement Ratios Between Greenhouse Gases and Pollutants

Measurements recorded at the UOU site from December 2015 to February 2016 are shown in Figure 3. The 6–16 February 2016 episode ("Valentine's event") was the longest episode of this season exhibiting the different stages (Baasandorj et al., 2017) and will be examined in greater detail in section 3.4. In this section we examine the relationships between excess concentrations after subtracting the baseline.

Figures 4a–4d and Table 2 show the scatterplots and regression slopes between CO_{2ex} and the excess concentrations of NAAQS species (CO_{ex}, NO_{xex}, and $PM_{2.5ex}$) during non-PCAP (green), Buildup (black), and PCAP (blue) periods. Robust relationships ($r^2 >= 0.65$) were observed between CO_{2ex} and several other measured coemitted gaseous pollutants at UOU during all PCAP phases (Figure 4 and Table 2). A consistent slope was observed between CO_{ex} and CO_{2ex} (ppb:ppm) during the different meteorological conditions during PCAP and Non-PCAP periods—that is, 7.19 and 8.87, respectively. This is not unexpected due to the relatively long lifetime for CO (approximately a few months) (Jacob, 1999; Sander et al., 2015) with respect to the residence time in the valley (several days during PCAPs) and numerous sources in which both species are coemitted. These slopes are comparable to those observed by Bush (2013), who reported slopes ranging from 5.2 to 9.1 in different parts of the SLV using on-road mobile measurements.

Observations of CO_{ex}:CO_{2ex} measurements performed at UOU throughout the study period resulted in a slope of 7.38 (ppb:ppm). This is a similar ratio as observed in other North American cities. For example, in spring of 2009 Sacramento had an observed ratio of 9.0–14.0 depending on whether the or not the CO_2 is constrained to only fossil fuel emissions (Turnbull, Karion, et al., 2011), with Indianapolis at 8.0 between 2012 and 2014 (Turnbull et al., 2015) and Los Angeles from October 2007 to February 2008 at 6.5 to 10 depending on the time of day and week (Djuricin, Pataki, & Xu, 2010).

Observed ratios in less developed countries where severe air quality events are more prevalent tend to be significantly higher, as the technologies driving combustion efficiency tend to be older and regulations less stringent. Turnbull, Tans, et al. (2011) found a CO:CO_2 ratio of 39 ppb:ppm for Shangdianzi, China from 2009 to 2010. Silva et al. (2013) used satellite retrievals from June 2009 to May 2010 to estimate CO and CO_2 emission factors of cities around the globe and compared those results to total column measurements and existing literature. They found significantly lower CO:CO_2 ratios in developed cities indicating that more developed nations have a higher efficiency of combustion. Their estimates ranged from 5.5 in Essen Germany to 47.6 in Beijing/Tianjin, China, with many of the developed cities at or below a ratio of 12. More recently, over the entire year of 2014 Super et al. (2017) found a value of 3.9 (ppb:ppm) in the inner city of Rotterdam, Netherlands, which they note is relatively clean compared to many existing estimates. Thus, the observed value of 7.38 for the CO_{ex}:CO_{2ex} ratio in the SLV fit well with other studied developed cities.

Even stronger correlations were observed between NO_{xex} and CO_{2ex} with a slope of 0.91, 0.90, and 1.01 and r^2 values of 0.90, 0.91, and 0.84 for the full sample period, Non-PCAP period, and PCAP period, respectively (Figure 4 and Table 2). Similar to CO, NO_x and CO_2 are coemitted from broadly similar sources; however, the tropospheric lifetime of NO_x is short compared to CO, measured on a time scale of days (Lopez et al., 2013), and plays a key role in the cycling of atmospheric radicals and secondary aerosol formation in the atmosphere (Finlayson-Pitts, 2011; Jacob, 1999) through the formation of species such as nitric acid (Baasandorj et al., 2017) (see below). The adoption of the 24 h running average baseline results in a comparison of recent urban emissions; thus, chemical loss plays less of a role in the NO_{xex}:CO_{2ex} relationship than if a conventional background had been selected. Thus, our selection of baseline likely drives the similarity in NO_{xex}:CO_{2ex} ratios during all phases of PCAPs (Figure 4b). Had a traditional background been applied in this comparison, chemical loss would have played a greater role, resulting in weaker relationships.

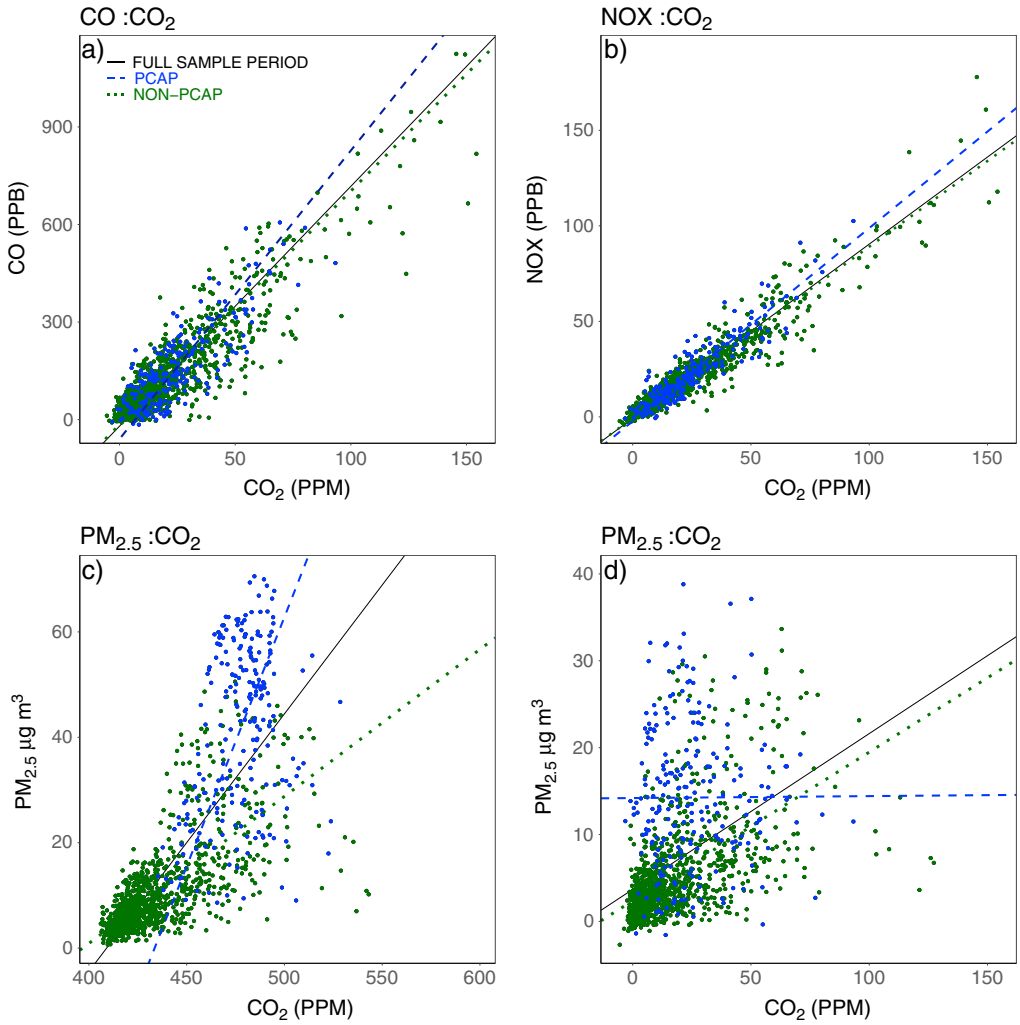

Figure 4. Multispecies linear regressions with full sample slope (black solid line), persistent cold air pool (PCAP) observations (blue dots, gray shaded regions in Figure 3) and slope (blue dashed line) and Non-PCAP observations (green dots) and slope (green dotted line) with (a) CO excess mixing ratio to CO_2 excess mixing ratio, (b) NO_x excess mixing ratio to CO_2 excess mixing ratio, (c) $PM_{2.5}$ mass concentration to CO_2 mixing ratio, (d) $PM_{2.5}$ excess mass concentration to CO_2 excess mixing ratio. Note that panel (c) is not excess concentrations. Values for slopes and correlation coefficient of each relationship is reported in Table 2. The strength of CO_2 as a proxy for the presence of coemitted pollutants is particularly noticeable in the trace gas relationships in panels (a) and (b).

As described in detail in section 3.4, long-lived PCAP episodes in the SLV have distinct phases including Buildup and Plateau phases (Figure 7). As NO_x accumulates in the valley over time during pollution episodes, the system is more oxidant limited during the Plateau period (Baasandorj et al., 2017), potentially resulting in a reduced loss rate of NO_x due to its oxidation. If this mechanism had been the main loss process determining the lifetime of NO_x, the NO_{xex} and CO_{2ex} ratio would have increased during the Plateau period compared to the ratio during the Buildup. The notably similar ratios during all phases of the PCAP examined in the study may indicate the importance of loss processes such as atmospheric transport in parallel with chemical loss, suggesting that transport could be still important during strong PCAP events. Transport could be occurring through movement of air masses between connecting valleys (i.e., Utah Valley to the south) or the Great Salt Lake (Figure 1), as well as mixing from aloft through turbulence or as air cools and descends into the upper layers of the PCAP.

The published literature containing direct measurements of both CO_2 and NO_x is limited and usually focused on a single source, for example, power plants (Lindenmaier et al., 2014) or traffic (Ammoura et al., 2014). The

fuel source and combustion technologies employed will greatly impact the observed ratio. For instance, Lindenmaier et al. (2014) measured plumes from coal fired power plants in the United States and found NO_x:CO_2 ratios of 1.5 (ppb:ppm). Ammoura et al. (2014) utilized high-traffic tunnels as a capture for on-road emissions in Paris and have identified a NO_x:CO_2 ratio of 6.5, though these authors note that European vehicles rely more heavily on diesel fuel than the United States resulting in higher observed emission ratios. Direct comparisons of urban atmospheric NO_x:CO_2 performed in Paris during winter of 2010 found highly similar ratios with variability related to origin of air mass (Lopez et al., 2013). Recent studies have utilized satellite retrievals to analyze trends in NO_x:CO_2 emission ratios (Reuter et al., 2014). They found that the NO_x:CO_2 ratios in Europe and North America are substantially lower than those in East Asia, but as East Asia adopts and implements new emission controls and renewed technologies they are experiencing a negative trend in the emission ratio; thus, NO_x emissions relative to CO_2 are decreasing, as expected (Reuter et al., 2014).

When compared to the few reported examples of direct simultaneous measurements of NO_x and CO_2, the low observed NO_{xex}:CO_{2ex} ratio of 0.91 (ppb:ppm) in the SLV is not surprising. This is due in part to the fact that the fuel sources of home heating and transportation in the SLV, predominantly natural gas and gasoline, respectively, release less NO_x than the coal and diesel fuel discussed in the literature above. Additionally, the removal of NO_x through oxidation results in a lower observed atmospheric emission ratio. As with CO and primary $PM_{2.5}$, as new combustion technologies are implemented and a greater proportion of energy consumption moves to renewable energies the NO_x:CO_2 ratio of the SLV should decrease. For example, the introduction of the Clean Air Act and implementation of stricter nitrogen oxide emission controls by the U.S. Environmental Protection Agency in the 2000s has resulted in a nationwide decrease of NO_x by 49% from 1990 to 2013. Nationwide NEI estimates for NO_x similarly decreased by 13% from 2008 to 2011 (Integrated Science Assessment, 2016). Other studies looking at specific emission sources have found decreases with increased combustion technologies. McDonald et al. (2012) estimated that gasoline engine NO_x emissions in California have decreased by 65% from 1990 to 2010.

The relationship reported in Table 2 between $PM_{2.5}$ and CO_2 $\mu g/m^3$:ppm explored in the long-term data set seen in Figure 2c as well as the winter 2015–2016 data in Figure 4c are different than those reported in Figure 4d. This is due to the fact that these do not have a baseline or background applied, while the latter does. Thus, the relationships explored are different, with a higher correlation during PCAPs expected between $PM_{2.5}$ and CO_2 than between $PM_{2.5ex}$ and CO_{2ex} as a result of coaccumulated pollutants during PCAPs. Additionally, the long-term relationship includes seasons other than wintertime, where primary particulate matter is dominant, and thus, the relationship is driven more by the coemission of $PM_{2.5}$ and CO_2.

Correlations with r^2 values of 0.56, 0.57, and 0.47 were found between $PM_{2.5}$ and CO_2 during full sample, PCAP, and Non-PCAP periods, respectively (Figure 4c). These correlation coefficients are similar to those observed during the long-term data set explored in section 3.1 as well as those observed in Portland Oregon (Rice & Bostrom, 2011). The lower correlation during PCAP conditions can be attributed to a higher contribution of primary organics to $PM_{2.5}$ mass (~30%) under Non-PCAP conditions compared to ~20% contribution during PCAPs (SIP, 2014). This difference in percentages is largely attributed to the fact that during PCAP conditions the secondary production of $PM_{2.5}$ increases mass concentrations significantly, resulting in a lower total observed percentage of primary $PM_{2.5}$. The primary component of $PM_{2.5}$ in the SLV during winter is ammonium nitrate (NH_4NO_3), which is formed in the atmosphere through an acid-based reversible reaction between gaseous ammonia (NH_3) and nitric acid (HNO_3). HNO_3 is formed in the atmosphere from NO_x reacting with O_3 (nocturnal) or an OH radical (daytime). While the relative contributions are still unknown, these two different pathways allow for the chemical loss of NO_x and the production of secondary organic aerosols that can occur in the SLV regardless of time of day (Baasandorj et al., 2017; Kelly et al., 2013).

Although there is a weak correlation between $PM_{2.5}$ and a stable tracer like CO_2, when the baseline is subtracted no correlation was found between corresponding excess concentrations $PM_{2.5ex}$ and CO_{2ex} during PCAP conditions. As a PCAP evolves, pollutants emitted from various sources accumulate within the shallow boundary layer; hence, they are all somewhat correlated (Figure 2). However, as pollutants accumulate, they undergo chemical transformations, leading to an increase in secondary $PM_{2.5}$. The observed lack of correlation between $PM_{2.5ex}$ and CO_{2ex} during PCAP conditions is consistent with the different sources of CO_2 and

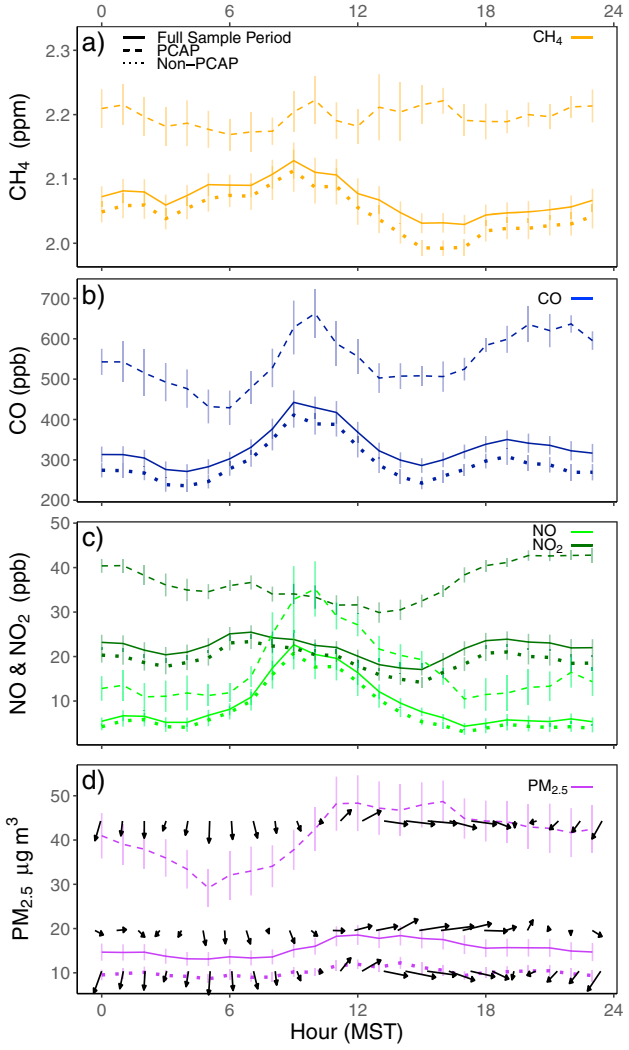

Figure 5. Diurnal cycles from University of Utah of (a) CH_4 mixing ratio, (b) CO mixing ratio, (c) mixing ratio of NO and NO_2, and (d) PM $_{2.5}$ mass concentration. Solid line indicates the full sample period from 27 December 2015 to 29 February 2016, dashed lines indicate periods of persistent cold air pools (PCAPs), and dotted lines Non-PCAP periods. Wind vectors are shown in panel (d) with arrows above the corresponding sample subset. The consistently elevated concentrations of all species during PCAP conditions is noticeable.

$PM_{2.5}$. Baasandorj et al. (2017) indicated that the aerosol nitrate formation takes place in the upper part of the boundary layer during a PCAP at night and the daytime mixing disperses the aerosol-rich air throughout the valley, contributing to the near-surface enhancements in $PM_{2.5}$. This results in a diurnal pattern of $PM_{2.5}$ substantially different from those of primary pollutants as discussed in detail in section 3.3 below and shown in Figures 5 and 6. Thus, a potentially useful metric is comparing baseline values, which results in a coefficient of 0.92 (Table 2).

Like CO_2, CH_4 is relatively stable, but unlike CO_2, CH_4 is not predominantly a product of combustion. Within urban environments CH_4 emissions are dominated by fugitive emissions from natural gas infrastructure and biological decomposition, the latter of which may be limited during wintertime. CH_{4ex}-to-tracer relationships are very similar to those observed with CO_2, indicating that elevated concentrations of stable tracers, regardless of source, are good indicators of accumulated pollutants during PCAP conditions (Table 2).

3.3. Diurnal Cycles of Greenhouse Gases (CO_2 and CH_4) and Pollutants

During Non-PCAP conditions and the full sample period, all trace gases exhibit a diurnal cycle similar to those observed by McKain et al. (2012) and Strong et al. (2011), (Figures 5 and 6). A morning maximum is observed due to emissions and transport and decreased concentrations during daytime driven by the CBL where mixing dilutes pollutants, followed by elevated concentrations at night due to the formation of a stable nocturnal boundary layer that traps the surface emissions. A tight connection between the urban emissions and transport processes can be seen in the observed diurnal profiles across different sites. As seen in Figures 6 and 7, CO_2 throughout the valley exhibits a similar pattern, but the range, baseline concentrations, and timing of the morning peak vary greatly depending on location. Sites deeper in the valley and closer to emission sources record higher concentrations (SUG and UOU) earlier, and those located farther from the urban influences and at higher elevations see substantially lower concentrations (DBK, SUN) later in the day. During PCAPs, this time lag is often greater due to more stable conditions, and CO_2 concentrations at SUN and DBK exhibits an inverted diurnal profile unlike the urban sites as discussed below. As shown in Figure 6b, CO_2 peaks at SUG around 8 a.m. reaching values as high as 490 and 550 ppm during non-PCAP and PCAPs, respectively. Emitted pollutants get transported across the valley then travel up to the sidewall and reach UOU at 9 a.m. and 10 a.m., respectively, during non-PCAP and PCAPs, and DBK at 11 a.m. during PCAPs as shown in Figure 6. At the UOU, peak values around ~ 460 and 490 ppm are observed, lower than those seen at SUG, during non-PCAP and PCAPs, respectively. The development of a shallow surface-based CBL distributes the pollutants throughout the CBL and leads to the observed decrease in CO_2 and increase in $PM_{2.5}$ by ~11 a.m. (Figure 5), consistent with the observations of Baasandorj et al. (2017). SUN, which is located outside the nocturnal boundary layer, sees the urban pollution only after the development of CBL; hence, CO_2 at SUN exhibits discernable enhancements during the day with a maxima of ~ 450 ppm around 1 p.m. during PCAPs. Consistent with a well-mixed CBL, CO_2 levels are similar across the sites during the day.

$PM_{2.5}$ shows a different pattern than CO_2 and CH_4 at UOU, reflecting different origins of these species (Figures 5d and 6). Due to the nighttime accumulation in the upper layers of a PCAP followed by the mixing during the day, $PM_{2.5}$ exhibits a diurnal profile with a daytime maxima ~ 10–11 a.m. and lower levels at night at the surface. This pattern is greatly accentuated as concentrations increase during the Buildup and PCAP

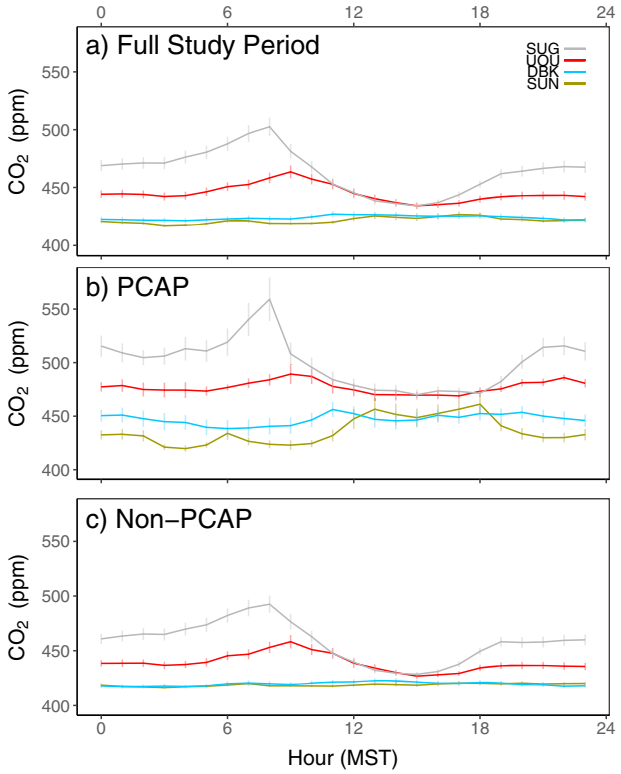

Figure 6. CO_2 mixing ratio from Sugarhouse (SUG, gray), University of Utah (UOU, red), Daybreak (DBK, blue), and Suncrest (SUN, gold) during (a) full sample period, (b) persistent cold air pool (PCAP) conditions, and (c) Non-PCAP conditions. This figure illustrates the differences in daily CO_2 mixing ratio patterns dependent on the location.

phases (see section 3.4). Lower concentrations in all observed species at UOU occur during the midnight to early morning hours. The concentration drops correspond to more northerly and easterly wind directions (Figure 5d), hinting at the role of downslope circulations at the northeasterly sidewall location of the UOU site (Figure 1). Similarly, Baasandorj et al. (2017) have shown stronger winds from easterly direction at night that corresponded with ozone (O_3) concentration increases.

3.4. Case Study: 6–16 February 2016 Episode

Throughout the sample period, five events that met our PCAP criteria (section 2.4) took place in SLV, each with elevated $PM_{2.5}$ and trace gas concentrations. The majority of these events were relatively short lived, with the exception of the event that lasted from 6 to 16 February 2016 (Figure 7). Consistent with other long-lived episodes in the SLV, this event showed three distinct periods: (1) a Buildup period between 6 and 10 February 2017, during which $PM_{2.5}$ concentration increased with a rate of ~7 $\mu g/m^3$; (2) a Plateau period (11–14 February 2016) when $PM_{2.5}$ fluctuates around 24-h $PM_{2.5}$ of 60 $\mu g/m^3$, evident by the peak of the baseline constraint; (3) a "Breakup" of the PCAP on 14 February resulting from the combination of cold-air advection aloft and stronger flow associated with the passing of a short-wave trough and strong surface heating, as seen in Figure 7.

Figure 7 shows the time series of trace gases and $PM_{2.5}$ at the UOU site, along with CO_2 at different sites in the SLV. Figure 8 shows the diurnal patterns of the species at UOU during the Buildup (solid) and Plateau (dashed) and wind vectors shown in Figure 8b. Figure 9 shows vertical profiles of potential temperature from the morning (05:00 MST) and afternoon (17:00 MST) radiosondes launched from the Salt Lake City International Airport for representative days during the Buildup (9 February) and Plateau (12 February) stages.

During the Buildup period, a corresponding increase in chemically stable gases (CH_4, CO_2) was seen throughout the valley (UOU, SUG, DBK, and SUN), with distinct patterns depending on the location of the observation site (Figure 7a). As with $PM_{2.5}$, a Plateau in CO_2 baseline concentrations was reached at around 475 ppm at UOU and DBK, but the timing of the Plateau depended on the location of the observation (Figure 7).

CO_2 at UOU started leveling off around same time when 24-hr $PM_{2.5}$ reached 60 $\mu g/m^3$ and began to stabilize. As PCAP conditions persisted in the SLV, CO_2 concentrations at the DBK site, situated at the edge of the urban dome and at a similar elevation to UOU, leveled off on 12 February, a day after UOU. Finally, CO_2 at SUN appears to show a small yet steady buildup initially, but it never reached a plateaued level due to its elevation. Instead, SUN exhibits very pronounced diurnal variation that oscillated between low concentrations at night similar to the background levels at HDP and high levels similar to the threshold CO_2 levels observed at UOU and DBK during the day (Figures 6 and 7). SUN is located ~500 m above the valley floor and was above the cold-pool, consistent with the observed low concentrations at night. Elevated concentrations were only observed during the daytime, when daytime heating mixed air with elevated concentrations to the site. The lagged increase in CO_2 concentrations observed at DBK compared to UOU (Figure 7) is consistent with the findings from Pataki et al. (2005), which found that during PCAP events in the SLV, urban air parcels with elevated CO_2 concentrations mix throughout the valley.

As indicated by Figure 9a, during PCAP Buildup conditions, the cold pool is stably stratified at night, and daytime surface heating is not sufficient for a convective layer to extend to the cold-air pool top but is limited to the lowest 200 m. During the Plateau stage, with a cloud-topped cold-pool in place, a different temperature structure is observed. The amplitude of the diurnal temperature cycle is greatly reduced, and a well-mixed layer, 350 m deep, is capped by a strong capping inversion. Cloud-top cooling is likely

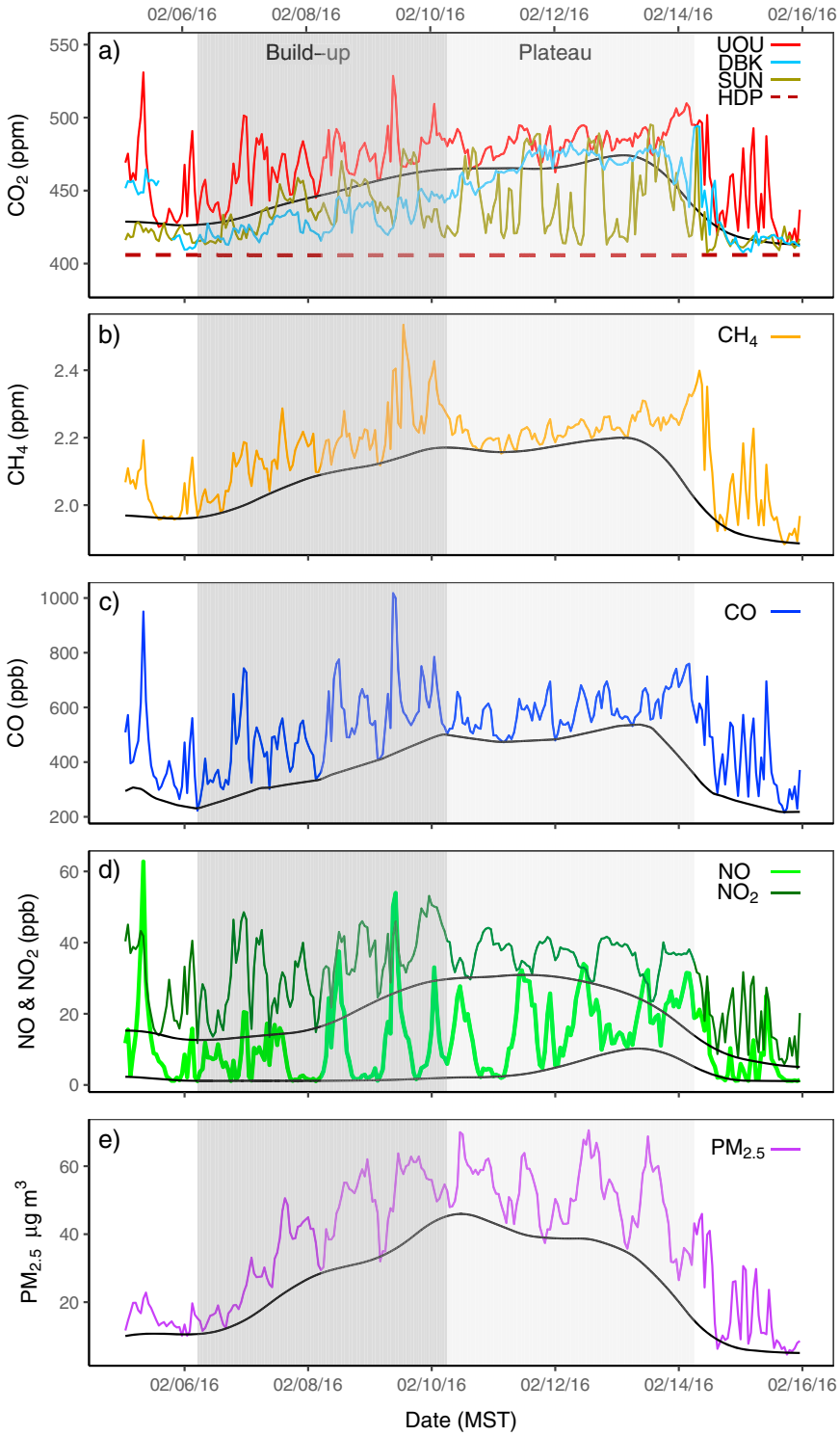

Figure 7. Time series of Valentine's event with the PCAP Buildup indicated in dark gray shaded region and Plateau indicated in light gray shaded region. (a) CO_2 mixing ratio from University of Utah (UOU) (red), Daybreak (DBK) (blue), Suncrest (SUN) (gold) and Hidden Peak (HDP) (dark red), with UOU observations of (b) CH_4 mixing ratio, (c) CO mixing ratio, (d) mixing ratio of NO and NO_2, and (e) $PM_{2.5}$ mass concentration. Black lines indicate calculated baseline. The Buildup period is characterized by increasing baseline concentrations of CO_2, CH_4, CO, and $PM_{2.5}$ with larger diurnal cycles, followed by the Plateau period characterized by a leveling off of baseline concentrations and a significant reduction in diurnal variability with the notable exception of $PM_{2.5}$. The clean-out event is very noticeable when all measured species at all sites decrease rapidly after the Plateau.

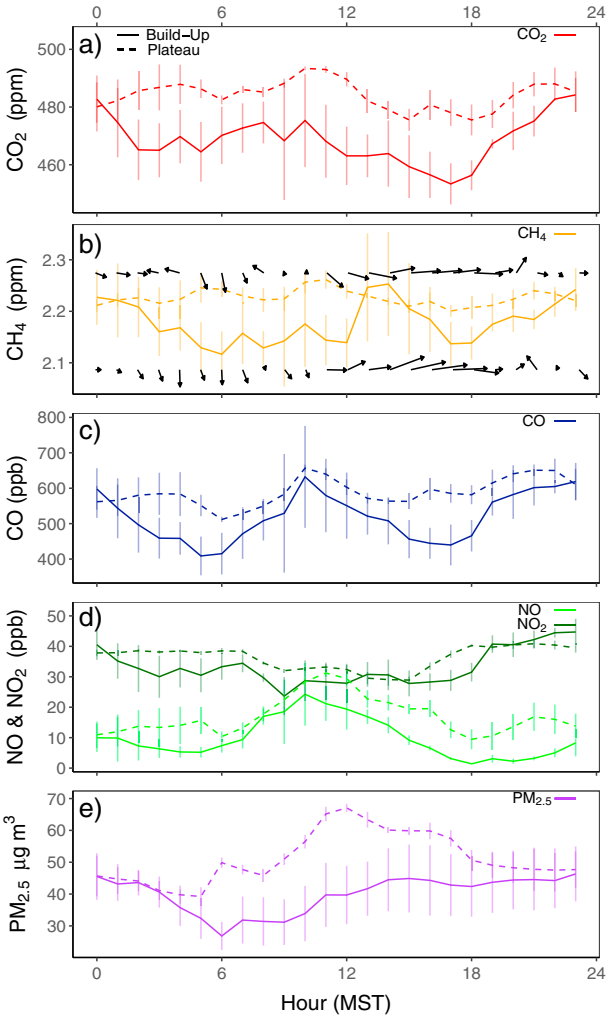

Figure 8. Diurnal cycles from University of Utah during the Valentine's event of (a) CO_2 mixing ratio, (b) CH_4 mixing ratio, (c) CO mixing ratio, (d) mixing ratio of NO and NO_2, and (e) $PM_{2.5}$ mass concentration. Solid line indicates the Buildup period, and dashed lines indicate Plateau. Wind vectors are shown in panel (b) with wind vector arrows corresponding to Stagnation period plotted above and the Buildup period plotted below.

playing an important role in producing cold air at the inversion top, which leads to a top-down convection in the lowest, near-surface layers. This likely leads to a more homogeneous distribution of pollutants within the PCAP. This is supported by the distinct differences in the diurnal trace gas patterns during the two phases. The amplitude of concentrations observed on a diurnal scale in all trace gas species is comparable to those observed during Non-PCAP and the other short lived PCAP events; however, during the Plateau stage the amplitude of daily trace gas concentrations is significantly reduced while maintaining a consistently elevated level (Figures 7 and 8). This is due to the well-mixed conditions that develop in the cloud topped cold pool during Plateau conditions (Figure 9b). This well-mixed condition with high NO_x at night can titrate O_3 throughout a large portion of a PCAP and in turn limit the particulate nitrate formation, leading to the plateau in $PM_{2.5}$ observed later in the episode. In contrast, stably stratified conditions during Buildup period decouples the surface emissions from the upper part of a PCAP, thus creating more favorable conditions for aerosol nitrate formation with lower NO_x and higher O_3 and leading to enhancements in $PM_{2.5}$ (Baasandorj et al., 2017).

As mentioned in section 3.2, the loss of NO_x through oxidation and the formation of secondary $PM_{2.5}$ can occur in the SLV through day and nighttime processes, but the proportion of each of these processes is not well understood. Thus, a better understanding of these processes may help highlight some of the diurnal patterns observed here. However, by calculating our baseline using a 24 h moving window, some of this uncertainty may be removed. This analysis further emphasizes the importance of interactions between the chemistry that drives the aerosol nitrate formation and the meteorological processes governing the stable stratification at night near surface and mixing of the pollutants within a PCAP during pollution episodes.

The stabilization of CO_2 concentrations observed along with the Plateau in $PM_{2.5}$, NO_x, and CO during the Valentine's event suggest that while atmospheric chemistry is likely the leading role in the observed patterns of $PM_{2.5}$ concentrations, atmospheric mixing across the PCAP top may be playing, at least to some extent, a role in the Plateau stage (Baasandorj et al., 2017). The Plateau period is characterized by a leveling off of baseline concentrations and a significant reduction in diurnal variability with the notable exception of $PM_{2.5}$. The clean-out event is very noticeable when all measured species at all sites decrease rapidly after the Plateau.

3.5. County-Wide Emission Ratios From Inventories

The emission ratio of CO_2 with different pollutants often varies with emission sources. While CO_2 estimates from top down emission inventories are generally well constrained, with uncertainty ranging from 3% to 40% depending on spatial scale and assimilation methods (Boden et al., 2009; Gurney et al., 2009; Peylin et al., 2009), the unique emission signatures from each source can lead to high uncertainty when estimating other trace gases and pollutants. This is due to varying combustion efficiencies, fuel types, and emission reduction technologies. For example, Turnbull, Tans, et al. (2011) compared the ratio of measured fossil fuel-derived CO_2 with another comeasured trace gas (CO) against available emission inventories and found differences ranging from 200 to 500%. Despite the uncertainties in emission inventories, they are a critical tool for identifying and implementing targeted emission regulations. Thus, by comparing inventory ratios to direct observations we can better understand the uncertainties and begin to improve on existing inventories.

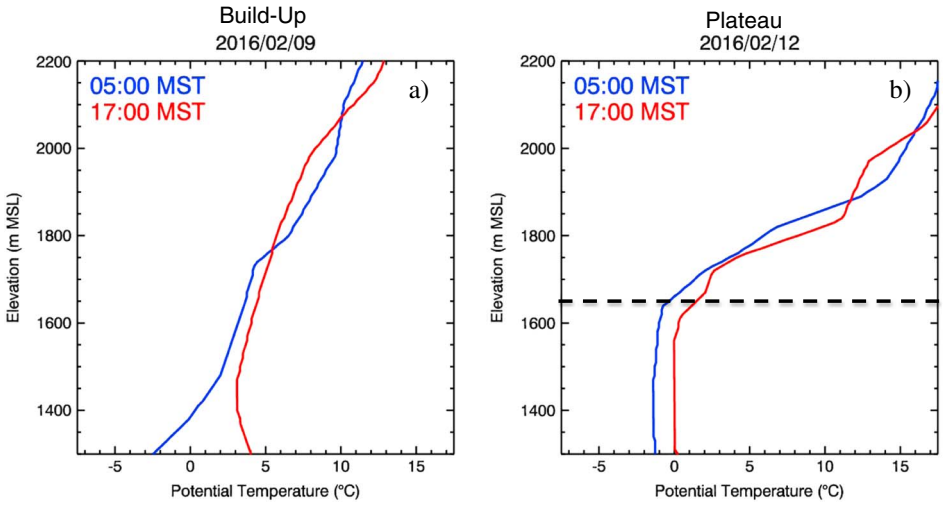

Figure 9. Vertical profiles of potential temperature from 5:00 MST (blue) and 17:00 MST (red) radiosondes launched from the Salt Lake City International Airport during (a) Buildup (ninth) and (b) Plateau (twelfth) stages. During PCAP Buildup conditions, the cold pool is stably stratified at night, and daytime heating is insufficient for a convective layer to extend to the cold-air pool top but is limited to the lowest 200 m. During the Plateau stage, a well-mixed layer (top marked by dashed line in panel (b) is capped by a strong capping inversion. The base of the capping inversion identified during Plateau by dashed black line in panel (b).

The emission ratios of CO:CO_2 and NO_x:CO_2 from the emission inventories in the SLV led to slopes of 9.56 and 2.73 millimoles/moles, respectively. In comparison, the observed CO_{ex}:CO_{2ex} slope of 7.38 (ppb:ppm) indicates that the inventories are slightly overestimating the county wide winter time emission ratio by a factor of 1.3. In contrast, the observed NO_{xex}:CO_{2ex} slope of 0.91 (ppb:ppm) indicates significant overestimation of the ratio by the emission inventory, by a factor of 3.0.

The small overestimation of CO:CO_2 and larger overestimation of NO_x:CO_2 emission ratios by the emission inventories is likely the result of several reasons. First, the sampling location of UOU is located well above the valley floor and removed from dense on-road, commercial, and industrial areas of the valley, and thus is probably subjected to less polluted air than other parts of the valley covered in the emission inventory. This is supported by Figure 6, where nighttime concentrations of CO_2 at SUG are consistently elevated above that of UOU. Second, residential emissions of CO_2 within the Hestia inventory do not include a source from wood burning while the NEI inventory incorporates this source within CO and NO_x emissions. Thus, the resulting ratios could be overestimated. Finally, as discussed in sections 3.3, advancements in combustion efficiency and the adoption of renewable technologies in North America and other industrialized nations have resulted in cleaner emissions which emission inventories have failed to accurately account for. The two-year difference between when the emission inventory was released and this measurement campaign could account for some of the observed difference. Indeed, this finding is consistent with much of the existing literature, which finds overestimation by the NEI of CO and NO_x emissions (Anderson et al., 2014; Brioude et al., 2013; Castellanos et al., 2011; Fujita et al., 2012; Yu et al., 2012).

In addition to the potential sources of overestimations discussed above, during PCAPs it is possible that individual emission sectors vary as temperatures decrease and heating demands in residential and commercial buildings increase. This is particularly true in the SLV where the overwhelming majority of heating is the result of natural gas combustion. This is supported by the higher observed slopes in CO:CO_2 and NO_x:CO_2 during PCAPs (Figure 4, Table 2). A detailed examination of the temporal variability in emission estimates could help to validate this but is beyond scope of our county wide, wintertime analysis conducted here.

4. Conclusions

Long-term measurements of CO_2 and $PM_{2.5}$ spanning 10 years show a high degree of correlation across all seasons in the Wasatch Front with some scatter around the mean. As indicated by the colocated

measurements performed as part of the Salt Lake Valley Wintertime $PM_{2.5}$ Study, some of this variance can be attributed to the meteorological conditions and whether or not those conditions are favorable for the secondary production of $PM_{2.5}$.

Greenhouse gases and criteria pollutants exhibited significant dynamic ranges in concentrations as the urban SLV undergoes different phases of wintertime PCAP events. Through this analysis we find excess CO_2 concentrations above the urban baseline (CO_{2ex}) to be a useful indicator of several criteria pollutants. CO_{2ex} shows strong and consistent relationships with coemitted trace gases (CO and NO_x) during all phases of wintertime atmospheric conditions examined in this study—that is, Non-PCAP, PCAP, Buildup and Plateau conditions. Another stable greenhouse gas, CH_4, exhibits similar relationships, suggesting that it is also a good indicator of wintertime pollution in the SLV. These findings indicate that as targeted greenhouse gas reductions are achieved in the SLV, similar measureable reductions in NAAQS criteria pollutants should be expected.

As seen at the UOU site and in the long-term data set, CO_2 concentrations provide a reasonable indicator for $PM_{2.5}$, especially when primary particulate matter constitutes a higher fraction of the total mass. This relationship breaks down as PCAP conditions facilitate secondary atmospheric reactions that result in $PM_{2.5}$ formation. On the other hand, the baseline levels of CO_2 and $PM_{2.5}$ covary and build up through the different phases of PCAP events, suggesting that CO_2 still provides a useful metric for elevated particulate matter concentrations. Additionally, concentrations of gaseous species appear to be more influenced by local emissions while $PM_{2.5}$ is more spatially homogenous. This is evident by the varying concentrations of CO_2 during PCAP conditions observed at different UUCON sites, with the highest concentrations occurring at the lowest elevation site SUG, followed by UOU, then differing at DBK and SUN depending on the time of day, while Baasandorj et al. (2017) found nearly identical $PM_{2.5}$ concentrations at HW and the UOU site during the same sample period.

While CO_{2ex} has limitations in indicating the presence of $PM_{2.5}$ during PCAP conditions, as a stable tracer CO_{2ex} is able to help explain the underlying processes that result in the secondary chemical production versus transport of $PM_{2.5}$ observed during PCAP events. As demonstrated in the Valentine's event case study (section 3.4) and covered in detail in Baasandorj et al. (2017), the Buildup, Plateau, and ultimate peak concentrations of $PM_{2.5}$ in the SLV during PCAP events, are highly dependent on the available gaseous precursors and the availability of oxidants required to drive the secondary chemistry. The observed Plateau stage in NO_x, CO, and the highly chemically stable CO_2 indicate that while atmospheric chemistry is a significant component driving $PM_{2.5}$ variations, meteorological processes also play a role in the evolution and plateauing of pollutant concentrations during PCAP events. The extent to which transport is contributing to the $PM_{2.5}$ Plateau will require a more extensive modeling effort that lies beyond the scope of the current paper. However, our observations illustrate the value and potential role chemically passive greenhouse gas observations such as CO_2 and CH_4 can play in helping to predict $PM_{2.5}$ concentrations in the SLV during PCAP events.

Compared to CO:CO_2 emission signatures around the globe, the Salt Lake area is comparable to other cities in more developed nations, many of which do not experience the same NAAQS exceedances in fine particulate matter as the SLV. This demonstrates the important role local topography, meteorological conditions, and atmospheric chemistry play in determining the air quality challenges of the Wasatch Front.

When compared to our in situ measurements we find that current emission inventories are well constrained for CO to CO_2 in the SLV with an overestimation of 1.3 and are overestimating the ratio of NO_x to CO_2 emissions by a factor of 3.0. This overestimation is not surprising given the pace of the implementation of new emission control technologies in the developed world.

While CO_{2ex} serves as a good indicator of the presence of gaseous pollutants, and in some cases $PM_{2.5}$, the exact linear relationships will be spatially dependent as a result of significant variations in emission sources within an urban domain. In order to best leverage the existing trace gas infrastructure, more work is needed to understand and quantify these relationships at each measurement location. Mobile data (Hopkins et al., 2016) and high resolution emission inventories like Hestia (Gurney et al., 2009; Gurney et al., 2011) can help inform these relationships, but both of these products have specific uncertainties that limit their effectiveness. High quality, colocated measurements, both in and out of PCAP conditions, would be best used to capture these relationships and begin to utilize the long-term and spatially diverse CO_2 infrastructure that currently exists along the Wasatch Front and in other urban areas.

As Utah's population is projected to add 2.5 million residents by 2050 (Harbeke et al., 2014), the overwhelming majority (90%) of which will live in the urbanized region along the Wasatch Front, understanding how targeted reductions in greenhouse gases will impact local air quality is vital. The ability to accurately measure air pollutant and GHG distributions coupled with urban growth projections will allow for an understanding of present and future air quality impacts and the contributions to climate change.

Annually, 3 million global premature deaths are attributed to exposure to poor ambient air quality (IEA, 2015; WHO, 2014) making it the fourth deadliest threat to modern human health. The ability to measure air pollutants precisely with a network density significant enough to accurately measure exposure for large populations will be one of the greatest scientific challenges of the 21st century. As demonstrated in this paper, CO_2 serves as an excellent stable and geographically distinct indicator of the presence of NAAQS trace gas criteria pollutants. Further, the strong relationships observed between CO_2 and the other gaseous species, as well as the relationship between the Non-PCAP $PM_{2.5}$ and CO_2 suggest that CO_2 could serve as a better indicator of NAAQS pollutants in regions where PCAPs do not result in conditions favorable for the formation of secondary particulate matter. The use and expansion of existing CO_2 networks in urban environments, such as the one in the Salt Lake Area, could prove to be a valuable tool in this endeavor.

Acknowledgments

This research was supported by the Department of Energy (DOE) grant DESC0010624, the National Oceanic and Atmospheric Administration (NOAA) grant NA140AR4310178, and the Utah Division of Air Quality. Funding for S. W. H came from the Utah Department of Environmental Quality and NSF grant AGS 1723337. The support and resources from the Center for High Performance Computing at the University of Utah are gratefully acknowledged. NCAR is sponsored by the National Science Foundation. Real-time and historic measurements from all CO_2 sites presented in this study can be viewed at http://air.utah.edu. The observational data used in this study are available upon request from the corresponding author or can be downloaded at the U-ATAQ's data repository at https://air.utah.edu/data/. We are grateful to the following institutions for hosting UUCON CO_2 measurements used in this study: Draper City and the Salt Lake County Unified Fire Authority, Rio Tinto Kennecott, and Snowbird Ski Resort. We would also like to thank David Bowling, Maria Garcia, and Jim Ehleringer for their support of this research in so many ways, without which the continued efforts to run the UUCON network would not be possible. Finally, we are always grateful for the constructive comments from Jocelyn Turnbull and the two other reviewers that greatly improved the manuscript.

References

Ahmadov, R., Mckeen, S., Trainer, M., Banta, R., Brewer, A., Brown, S., et al. (2015). Understanding high wintertime ozone pollution events in an oil- and natural gas-producing region of the western US. *Atmospheric Chemistry and Physics*, *411*, 429. https://doi.org/10.5194/acp-15-411-2015

Ammoura, L., Gros, V., Baudic, A., et al. (2014). Atmospheric measurements of ratios between CO_2 and co-emitted species from traffic: A tunnel study in the Paris megacity. *Atmospheric Chemistry and Physics*, *14*(23), 12,871–12,882. https://doi.org/10.5194/acp-14-12871-2014

Anderson, D. C., Loughner, C. P., Diskin, G., Weinheimer, A., Canty, T. P., Salawitch, R. J., et al. (2014). Measured and modeled CO and NO_y in DISCOVER-AQ: An evaluation of emissions and chemistry over the eastern US. *Atmospheric Environment*, *96*, 78–87. https://doi.org/10.1016/j.atmosenv.2014.07.004

Andrews, A. E., Kofler, J. D., Trudeau, M. E., Williams, J. C., Neff, D. H., Masarie, K. A., et al. (2014). CO_2, CO, and CH_4 measurements from tall towers in the NOAA earth system research laboratory's global greenhouse gas reference network: Instrumentation, uncertainty analysis, and recommendations for future high-accuracy greenhouse gas monitoring efforts. *Atmospheric Measurement Techniques*, *7*(2), 647–687. http://doi.org/10.5194/amt-7-647-2014

Baasandorj, M., Hoch, S. W., Bares, R., Lin, J. C., Brown, S. S., Millet, D. B., et al. (2017). Coupling between chemical and meteorological processes under persistent cold-air pool Conditions: Evolution of wintertime $PM_{2.5}$ pollution events and N_2O_5 observations in Utah's Salt Lake Valley. https://doi.org/10.1021/acs.est.6b06603

Behera, S. N., Sharma, M., Aneja, V. P., & Balasubramanian, R. (2013). Ammonia in the atmosphere: A review on emission sources, atmospheric chemistry and deposition on terrestrial bodies. *Environmental Science and Pollution Research*, *20*(11), 8092–8131. https://doi.org/10.1007/s11356-013-2051-9

Boden, T. A., Marland, G., & Andres, R. J. (2009). Global, regional and national fossil-fuel CO_2 emissions, Carbon Dioxide Information Analysis Center, Oak Ridge National Laboratory, US Department of Energy, Oak Ridge, TN.

Brioude, J., Angevine, W. M., Ahmadov, R., Kim, S., Evan, S., Mckeen, S. A., et al. (2013). Top-down estimate of surface flux in the Los Angeles Basin using a mesoscale inverse modeling technique: Assessing anthropogenic emissions of CO, NO_x and CO_2 and their impacts. *Atmospheric Chemistry and Physics*, *13*(7), 3661–3677. https://doi.org/10.5194/acp-13-3661-2013

Brown, S. S., & Stutz, J. (2012). Nighttime radical observations and chemistry. *Chemical Society Reviews*, *41*(19), 6405–6447. https://doi.org/10.1039/c2cs35181a

Bush, S. (2013). "Spatiotemporal dynamics of CO and CO_2, Salt Lake Valley, Utah USA." American Geophysical Union Conference. December 2013, San Francisco. Presentation.

Butz, A., Guerlet, S., Hasekamp, O., Schepers, D., Galli, A., Aben, I., et al. (2011). Toward accurate CO_2 and CH_4 observations from GOSAT. *Geophysical Research Letters*, *38*, L14812. https://doi.org/10.1029/2011GL047888

Castellanos, P., Marufu, L. T., Doddridge, B. G., Taubman, B. F., Schwab, J. J., Hains, J. C., et al. (2011). Ozone, oxides of nitrogen, and carbon monoxide during pollution events over the eastern United States: An evaluation of emissions and vertical mixing. *Journal of Geophysical Research*, *116*, D16307. https://doi.org/10.1029/2010JD014540

Crisp, D., Fisher, B. M., O'Dell, C., Frankenberg, C., Basilio, R., Bösch, H., et al. (2012). The ACOS CO_2 retrieval algorithm—Part II: Global X_{CO2} data characterization. *Atmospheric Measurement Techniques*, *5*(4), 687–707. https://doi.org/10.5194/amt-5-687-2012

Djuricin, S., Pataki, D. E., & Xu, X. (2010). A comparison of tracer methods for quantifying CO_2 sources in an urban region. *115*(14), 1–13. https://doi.org/10.1029/2009JD012236

Dlugokencky, E. J., Myers, R. C., Lang, P. M., Masarie, K. A., Crotwell, A. M., Thoning, K. W., et al. (2005). Conversion of NOAA atmospheric dry air CH_4 mole fractions to a gravimetrically prepared standard scale. *Journal of Geophysical Research*, *110*, D18306. https://doi.org/10.1029/2005JD006035

Dolman, A. J., Noilhan, J., Durand, P., Sarrat, C., Brut, A., Piguet, B., et al. (2006). The CarboEurope regional experiment strategy. *Bulletin of the American Meteorological Society*, *87*(10), 1367–1380. https://doi.org/10.1175/BAMS-87-10-1367

Duren, R. M., & Miller, C. E. (2012). Measuring the carbon emissions of megacities. *Nature Climate Change*, *2*(8), 560–562. https://doi.org/10.1038/nclimate1629

Finlayson-Pitts, B. J. (2011). *Chemistry of the upper and lower atmosphere: theory, experiments and applications*. San Diego, CA: Academic Press.

Foster, C. S., Crosman, E. T., Holland, L., Mallia, D. V., Fasoli, B., Bares, R., et al. (2017). Confirmation of elevated methane emissions in Utah's Uintah Basin with ground-based observations and a high-resolution transport model. *Journal of Geophysical Research: Atmospheres*, *122*, 1–19. https://doi.org/10.1002/2017JD027480

Fujita, E. M., Campbell, D. E., Zielinska, B., Chow, J. C., Lindhjem, C. E., Denbleyker, A., et al. (2012). EMFAC2007 mobile source emission models with on-road traffic tunnel and remote sensing measurements mobile source emission models with on-road traffic tunnel and remote sensing measurements. *Journal of the Air & Waste Management Association*, *62*(10), 1134–1149. https://doi.org/10.1080/10962247.2012.699016

Gillies, R. R., Wang, S.-Y., & Booth, M. R. (2010). Atmospheric scale interaction on wintertime intermountain west low-level inversions. *Weather and Forecasting*, *25*(4), 1196–1210. https://doi.org/10.1175/2010WAF2222380.1

Gorski, G., Strong, C., Good, S. P., Bares, R., Ehleringer, J. R., & Bowen, G. J. (2015). Vapor hydrogen and oxygen isotopes reflect water of combustion in the urban atmosphere. *Proceedings of the National Academy of Sciences of the United States of America*, *112*(11), 3247–3252. https://doi.org/10.1073/pnas.1424728112

Green, M. C., Chow, J. C., Watson, J. G., Dick, K., & Inouye, D. (2015). Effects of snow cover and atmospheric stability on winter $PM_{2.5}$ concentrations in western U.S. valleys. *Journal of Applied Meteorology and Climatology*, *54*(6), 1191–1201. https://doi.org/10.1175/JAMC-D-14-0191.1

Gurney, K. R., Mendoza, D. L., Zhou, Y., Fischer, M. L., Miller, C. C., Geethakumar, S., & de la Rue du Can, S. (2009). High resolution fossil fuel combustion CO_2 emission fluxes for the United States. *Environmental Science & Technology*, *43*(14), 5535–5541. https://doi.org/10.1021/es900806c

Gurney, K. R., Zhou, Y., Mendoza, D., Chandrasekaran, V., Geethakumar, S., Razlivanov, I., et al. (2011). Vulcan and Hestia: High resolution quantification of fossil fuel CO_2 emissions. *MODSIM 2011 - 19th International Congress on Modelling and Simulation - Sustaining Our Future: Understanding and Living with Uncertainty*, (December), 1781–1787.

Harbeke, D. T., Garbett, B., Chairman, V., Matsumori, D., Kroes, S. J. H., & City, S. L. (2014). A snapshot of 2050, (720).

Hopkins, F. M., Kort, E. A., Bush, S. E., Ehleringer, J. R., Lai, C.-T., Blake, D. R., & Randerson, J. T. (2016). Spatial patterns and source attribution of urban methane in the Los Angeles Basin. *Journal of Geophysical Research: Atmospheres*, *10*, 2490–2507. https://doi.org/10.1002/2015JD024429.Received

Horel, J., Splitt, M., Dunn, L., Pechmann, J., White, B., Ciliberti, C., et al. (2002). Mesowest: Cooperative mesonets in the western United States. *Bulletin of the American Meteorological Society*, *83*(2), 211–225. https://doi.org/10.1175/1520-0477(2002)083%3C0211:MCMITW%3E2.3.CO;2

Integrated Science Assessment for Oxides of Nitrogen—Health Criteria Integrated Science Assessment for Oxides of Nitrogen—Health Criteria (2016). (January).

IEA (2015). Energy and Climate Change. *World Energy Outlook Special Report*, 1–200. http://doi.org/10.1038/479267b

Jacob, D. J. (1999). *Introduction to atmospheric chemistry*. New Jersey: Princeton University Press.

Kelly, K. E., Kotchenruther, R., Kuprov, R., Silcox, G. D., Kelly, K. E., Kotchenruther, R., et al. (2013). Receptor model source attributions for Utah's Salt Lake City Airshed and the impacts of wintertime secondary ammonium nitrate and ammonium chloride aerosol, *2247*(June 2017). *Journal of the Air and Waste Management Association*, *63*(5), 575–590. https://doi.org/10.1080/10962247.2013.774819

Kolb, C. E., Herndon, S. C., McManus, J. B., Shorter, J. H., Zahniser, M. S., Nelson, D. D., et al. (2002). Mobile laboratory with rapid response instruments for real-time measurements of urban and regional trace gas and particulate distributions and emission source characteristics. *Environmental Science & Technology*, *38*, 5694–5703.

Kondo, J., Kuwagata, T., & Haginoya, S. (1989). Heat budget analysis of nocturnal cooling and daytime heating in a basin. *Journal of the Atmospheric Sciences*, *46*(19), 2917–2933. https://doi.org/10.1175/1520-0469(1989)046%3C2917:HBAONC%3E2.0.CO;2

Kuprov, R., Eatough, D. J., Cruickshank, T., Olson, N., Paul, M., Hansen, J. C., et al. (2014). Composition and secondary formation of fine particulate matter in the Salt Lake Valley. *Journal of the Air & Waste Management Association*, *64*(8), 957–969. https://doi.org/10.1080/10962247.2014.903878

Lareau, N. P., Crosman, E., Whiteman, C. D., Horel, J. D., Hoch, S. W., Brown, W. O. J., & Horst, T. W. (2013). The persistent cold-air pool study. *Bulletin of the American Meteorological Society*, *94*(1), 51–63. https://doi.org/10.1175/BAMS-D-11-00255.1

Lauvaux, T., Miles, N. L., Deng, A., Richardson, S. J., Cambaliza, M. O., Davis, K. J., et al. (2016). High-resolution atmospheric inversion of urban CO_2 emissions during the dormant season of the Indianapolis Flux Experiment (INFLUX). *Journal of Geophysical Research: Atmospheres*, *121*, 5213–5236. https://doi.org/10.1002/2015JD024473

Legendre, P., & Legendre, L. (1998). *Numerical ecology* (2nd ed.). New York: Elsevier.

Lindenmaier, R., Dubey, M. K., Henderson, B. G., Butterfield, Z. T., Herman, J. R., Rahn, T., & Lee, S.-H. (2014). Multiscale observations of CO_2, $^{13}CO_2$, and pollutants at four corners for emission verification and attribution. *Proceedings of the National Academy of Sciences*, *111*(23), 8386–8391. https://doi.org/10.1073/pnas.1321883111

Long, R. W., Eatough, N. L., Mangelson, N. F., Thompson, W., Fiet, K., Smith, S., et al. (2003). The measurement of $PM_{2.5}$, including semi-volatile components, in the EMPACT program: Results from the Salt Lake City study. *Atmospheric Environment*, *37*(31), 4407–4417.

Lopez, M., Schmidt, M., Delmotte, M., Colomb, A., Gros, V., Janssen, C., et al. (2013). CO, NO_x and $^{13}CO_2$ as tracers for fossil fuel CO_2: Results from a pilot study in Paris during winter 2010. *Atmospheric Chemistry and Physics*, *13*(15), 7343–7358. http://doi.org/10.5194/acp-13-7343-2013

Malek, E., Davis, T., Martin, R. S., & Silva, P. J. (2006). Meteorological and environmental aspects of one of the worst national air pollution episodes (January, 2004) in Logan, Cache Valley, Utah, USA. *Atmospheric Research*, *79*(2), 108–122. https://doi.org/10.1016/j.atmosres.2005.05.003

Mcdonald, B. C., Dallmann, T. R., Martin, E. W., & Harley, R. A. (2012). Long-term trends in nitrogen oxide emissions from motor vehicles at national, state, and air basin scales. *Journal of Geophysical Research*, *117*, D00V18. https://doi.org/10.1029/2012JD018304

McKain, K., Wofsy, S. C., Nehrkorn, T., Eluszkiewicz, J., & Ehleringer, J. (2012). Assessment of ground-based atmospheric observations for verification of greenhouse gas emissions from an urban region. *Proceedings of the National Academy of Sciences*, *109*(22), 8423–8428. https://doi.org/10.1073/pnas.1116645109

Mitchell, L. E., Lin, J., Bowling, D., Pataki, D., Strong, C., Schauer, A., et al. (2018). Long-term urban carbon dioxide observations reveal spatial and temporal dynamics related to urban characteristics and growth. *Proceedings of the National Academy of Sciences*. https://doi.org/10.1073/pnas.1702393115

National Emissions Inventory (NEI) (2014). United States Environmental Protection Agency. https://www.epa.gov/air-emissions-inventories/national-emissions-inventory-nei

Newman, S., Xu, X., Affek, H. P., Stolper, E., & Epstein, S. (2008). Changes in mixing ratio and isotopic composition of CO_2 in urban air from the Los Angeles basin, California, between 1972 and 2003. *Journal of Geophysical Research*, *113*, D23304. https://doi.org/10.1029/2008JD009999

Newman, S., Xu, X., Gurney, K. R., Hsu, Y. K., Li, K. F., Jiang, X., et al. (2016). Toward consistency between trends in bottom-up CO_2 emissions and top-down atmospheric measurements in the Los Angeles megacity. *Atmospheric Chemistry and Physics*, *16*(6), 3843–3863. https://doi.org/10.5194/acp-16-3843-2016

Palmer, P. I., Suntharalingam, P., Jones, D. B. A., Jacob, D. J., Streets, D. G., Fu, Q., et al. (2006). Using CO_2:CO correlations to improve inverse analyses of carbon fluxes. *Journal of Geophysical Research*, *111*, D12318. https://doi.org/10.1029/2005JD006697

Panday, A. K., Prinn, R. G., & Schär, C. (2009). Diurnal cycle of air pollution in the Kathmandu Valley, Nepal: 2. *Modeling results*. *Journal of Geophysical Research Atmospheres*, *114*, 1–20. http://doi.org/10.1029/2008JD009808

Pataki, D. E., Bowling, D. R., & Ehleringer, J. R. (2003). Seasonal cycle of carbon dioxide and its isotopic composition in an urban atmosphere: Anthropogenic and biogenic effects. *Journal of Geophysical Research*, *108*(D23), 4735. https://doi.org/10.1029/2003JD003865

Pataki, D. E., Bowling, D. R., Ehleringer, J. R., & Zobitz, J. M. (2006). High resolution atmospheric monitoring of urban carbon dioxide sources. *Geophysical Research Letters*, *33*, L03818. https://doi.org/10.1029/2005GL024822

Pataki, D. E., Tyler, B. J., Peterson, R. E., Nair, A. P., Steenburgh, W. J., & Pardyjak, E. R. (2005). Can carbon dioxide be used as a tracer of urban atmospheric transport? *Journal of Geophysical Research*, *110*, D15102. https://doi.org/10.1029/2004JD005723

Pataki, D. E., Xu, T., Luo, Y. Q., & Ehleringer, J. R. (2007). Inferring biogenic and anthropogenic carbon dioxide sources across an urban to rural gradient. *Oecologia*, *152*(2), 307–322. https://doi.org/10.1007/s00442-006-0656-0

Patarasuk, R., Gurney, K. R., O'Keeffe, D., Song, Y., Huang, J., Rao, P., et al. (2016). Urban high-resolution fossil fuel CO_2 emissions quantification and exploration of emission drivers for potential policy applications. *Urban Ecosystems*, *19*(3), 1013–1039. https://doi.org/10.1007/s11252-016-0553-1

Peylin, P., Houweling, S., Krol, M. C., Karstens, U., Rödenbeck, C., Geels, C., et al. (2009). Importance of fossil fuel emission uncertainties over Europe for CO_2 modeling: Model intercomparison. *Atmospheric Chemistry and Physics Discussions*, *9*(2), 7457–7503. https://doi.org/10.5194/acpd-9-7457-2009

Pouliot, G., Keating, T., Maenhout, G., Chang, C., Beidler, J., & Cleary, R. (2014). The incorporation of the US National Emission Inventory into version 2 of the hemispheric transport of air pollutants inventory. In D. Steyn, & R. Mathur (Eds.), *Air pollution modeling and its application XXIII*, (pp. 265–268). Cham: Springer International Publishing.

Reuter, M., Buchwitz, M., Hilboll, A., Richter, A., Schneising, O., Hilker, M., et al. (2014). Decreasing emissions of NO_x relative to CO_2 in East Asia inferred from satellite observations. *Nature Geoscience*, *7*(11), 792–795. https://doi.org/10.1038/NGEO2257

Rice, A., & Bostrom, G. (2011). Measurements of carbon dioxide in an Oregon metropolitan region. *Atmospheric Environment*, *45*(5), 1138–1144. https://doi.org/10.1016/j.atmosenv.2010.11.026

Sander, S. P., Friedl, R. R., Golden, D. M., Kurylo, M. J., Moortgat, G. K., Wine, P. H., et al. (2015). Chemical kinetics and photochemical data for use in atmospheric studies evaluation number 15. *Cross Sections, California*, *15*, 1–153. https://doi.org/10.1002/kin.550171010

Sarrat, C., Noilhan, J., Lacarre, P., Donier, S., Lac, C., Calvet, J. C., et al. (2007). Atmospheric CO_2 modeling at the regional scale: Application to the CarboEurope Regional Experiment. *Journal of Geophysical Research*, *112*, D12105. https://doi.org/10.1029/2006JD008107

Silcox, G. D., Kelly, K. E., Crosman, E. T., Whiteman, C. D., & Allen, B. L. (2012). Wintertime $PM_{2.5}$ concentrations during persistent, multi-day cold-air pools in a mountain valley. *Atmospheric Environment*, *46*, 17–24. https://doi.org/10.1016/j.atmosenv.2011.10.041

Silva, P. J., Vawdrey, E. L., Corbett, M., & Erupe, M. (2007). Fine particle concentrations and composition during wintertime inversions in Logan, Utah, USA. *Atmospheric Environment*, *41*(26), 5410–5422. https://doi.org/10.1016/j.atmosenv.2007.02.016

Silva, S. J., Arellano, A. F., & Worden, H. M. (2013). Toward anthropogenic combustion emission constraints from space-based analysis of urban CO_2/CO sensitivity. *Geophysical Research Letters*, *40*, 4971–4976. https://doi.org/10.1002/grl.50954

SIP (2014). Utah State Implementation: Plan control measures for area and point sources, Fine Particulate Matter, $PM_{2.5}$ SIP for the Salt Lake City, UT Nonattainment Area; Utah Division of Air Quality: Salt Lake City, UT; http://www.deq.utah.gov/Laws_Rules/daq/sip/docs/2014/12Dec/SIP%20IX.A.21_SLC_FINAL_Adopted%2012-3-14.pdf (Last accessed: 11/2016).

Sokal, R. R., & Rohlf, F. J. (1995). Assumptions of analysis of variance. In *Biometry: The principles and practice of statistics in biological research*, (pp. 392–450). New York: W.H. Freeman and Company.

State Energy Data System (SEDS) (2016). 1960–2014 (complete), Energy Information Administration. http://www.eia.gov/state/seds/seds-data-complete.cfm?sid=US, last accessed: July 23, 2016.

Staufer, J., Broquet, G., Bréon, F.-M., Puygrenier, V., Chevallier, F., Xueref-Rémy, I., et al. (2016). A first year-long estimate of the Paris region fossil fuel CO_2 emissions based on atmospheric inversion. *Atmospheric Chemistry and Physics Discussions*, 1–34. https://doi.org/10.5194/acp-2016-191

Stelson, A. W., & Seinfeld, J. H. (1982). Relative humidity and temperature dependence of the ammonium nitrate dissociation constant. *Atmospheric Environment*, *16*(5), 983–992. https://doi.org/10.1016/0004-6981%20(82)90184-6

Stephens, B. B., Miles, N. L., Richardson, S. J., Watt, A. S., & Davis, K. J. (2011). Atmospheric CO_2 monitoring with single-cell NDIR-based analyzers. *Atmospheric Measurement Techniques*, *4*(12), 2737–2748. https://doi.org/10.5194/amt-4-2737-2011

Strong, C., Stwertka, C., Bowling, D. R., Stephens, B. B., & Ehleringer, J. R. (2011). Urban carbon dioxide cycles within the Salt Lake Valley: A multiple-box model validated by observations. *Journal of Geophysical Research*, *116*, D15307. https://doi.org/10.1029/2011JD015693

Super, I., Denier van der Gon, H. A. C., Visschedijk, A. J. H., Moerman, M. M., Chen, H., van der Molen, M. K., & Peters, W. (2017). Interpreting continuous in-situ observations of carbon dioxide and carbon monoxide in the urban port area of Rotterdam. *Atmospheric Pollution Research*, *8*(1), 174–187. https://doi.org/10.1016/j.apr.2016.08.008

Tans, P. P., Bakwin, P. S., & Guenther, D. W. (1996). A feasible global cycle observing system: A plan to decipher today's carbon cycle based on observations. *Global Change Biology*, *2*(3), 309–318. https://doi.org/10.1111/j.1365-2486.1996.tb00082.x

Turnbull, J., Guenther, D., Karion, A., Sweeney, C., Anderson, E., Andrews, A., et al. (2012). An integrated flask sample collection system for greenhouse gas measurements. *Atmospheric Measurement Techniques*, *5*(9), 2321–2327. https://doi.org/10.5194/amt-5-2321-2012

Turnbull, J. C., Karion, A., Fischer, M. L., Faloona, I., Guilderson, T., Lehman, S. J., et al. (2011). Assessment of fossil fuel carbon dioxide and other anthropogenic trace gas emissions from airborne measurements over Sacramento, California in spring 2009. *Atmospheric Chemistry and Physics*, *11*(2), 705–721. https://doi.org/10.5194/acp-11-705-2011

Turnbull, J. C., Sweeney, C., Karion, A., Newberger, T., Lehman, S. J., Cambaliza, M. O., et al. (2015). Toward quantification and source sector identification of fossil fuel CO_2 emissions from an urban area: Results from the INFLUX experiment. *Journal of Geophysical Research. Atmospheres*, *120*, 292–312. https://doi.org/10.1002/2014JD022555

Turnbull, J. C., Tans, P. P., Lehman, S. J., Baker, D., Conway, T. J., Chung, Y. S., et al. (2011). Atmospheric observations of carbon monoxide and fossil fuel CO_2 emissions from East Asia. *Journal of Geophysical Research: Atmospheres*, *116*, 1–14. https://doi.org/10.1029/2011JD016691

Ueyama, M., & Ando, T. (2016). Diurnal, weekly, seasonal and spatial variabilities in carbon dioxide flux in different urban landscapes in Sakai, Japan. *Atmospheric Chemistry and Physics Discussions*, *2*(June), 1–20. https://doi.org/10.5194/acp-2016-334

Vardag, S. N., Gerbig, C., Janssens-Maenhout, G., & Levin, I. (2015). Estimation of continuous anthropogenic CO_2: Model-based evaluation of CO_2, CO, $^{13}C(CO_2)$ and $^{14}C(CO_2)$ tracer methods. *Atmospheric Chemistry and Physics*, *15*(22), 12,705–12,729. https://doi.org/10.5194/acp-15-12705-2015

Villalobos-Pietrini, R., Amador-Muoz, O., Waliszewski, S., Hernndez-Mena, L., Munive-Coln, Z., Gmez-Arroyo, S., et al. (2006). Mutagenicity and polycyclic aromatic hydrocarbons associated with extractable organic matter from airborne particles ≤10 μm in southwest Mexico City. *Atmospheric Environment*, *40*(30), 5845–5857. https://doi.org/10.1016/j.atmosenv.2006.05.009

Wallington, T. J., Sullivan, J. L., & Hurley, M. D. (2008). Emissions of CO_2, CO, NO_x, HC, PM, HFC-134a, N_2O and CH_4 from the global light duty vehicle fleet. *Meteorologische Zeitschrift*, *17*(2), 109–116. https://doi.org/10.1127/0941-2948/2008/0275

Watson, R. T., Rodhe, H., Oeschger, H., & Siegenthaler, U. (1990). Greenhouse gases and aerosols. *Climate Change: The IPCC Scientific Assessment*, 1–40. Retrieved from http%3A%2F%2Fwww.scopus.com%2Finward%2Frecord.url%3Feid%3D2-s2.0-0025587274%26amp%3BpartnerID%3D40%26amp%3Bmd5%3D5d3e969d5d655f48f55e679627df52ab

Whiteman, C. D., Hoch, S. W., Horel, J. D., & Charland, A. (2014). Relationship between particulate air pollution and meteorological variables in Utah's Salt Lake Valley. *Atmospheric Environment*, *94*, 742–753. https://doi.org/10.1016/j.atmosenv.2014.06.012

Whiteman, C. D., Hoch, S. W., Lehner, M., & Haiden, T. (2010). Nocturnal cold-air intrusions into a closed basin: Observational evidence and conceptual model. *Journal of Applied Meteorology and Climatology*, *49*(9), 1894–1905. https://doi.org/10.1175/2010JAMC2470.1

WHO (2014). WHO's Ambient Air Pollution database - Update 2014 Data summary of the AAP database, 2–7. Retrieved from http://www.who.int/phe/health_topics/outdoorair/databases/cities/en

Wilkey, J., Kelly, K., Jaramillo, I. C., Spinti, J., Hogue, M., Pasqualini, D., et al. (2016). Predicting emissions from oil and gas operations in the Uinta Basin, Utah. *Journal of the Air & Waste Management Association*, *66*(5), 528–545. https://doi.org/10.1080/10962247.2016.1153529

Yokota, T., Yoshida, Y., Eguchi, N., Ota, Y., Tanaka, T., Watanabe, H., & Maksyutov, S. (2009). Global concentrations of CO_2 and CH_4 retrieved from GOSAT: First preliminary results. *Scientific Online Letters of the Atmosphere*, *5*, 160–163.

Yu, S., Mathur, R., Pleim, J., Pouliot, G., Wong, D., Eder, B., et al. (2012). Comparative evaluation of the impact of WRF-NMM and WRF-ARW meteorology on CMAQ simulations for O_3 and related species during the 2006 TexAQS/GoMACCS campaign. *Atmospheric Pollution Research*, *3*(2), 149–162. https://doi.org/10.5094/APR.2012.015

Zhao, C. L., & Tans, P. P. (2006). Estimating uncertainty of the WMO mole fraction scale for carbon dioxide in air. *Journal of Geophysical Research*, *111*, D08S09. https://doi.org/10.1029/2005JD006003

Erratum

In the originally published version of this article, there were several errors in Table 2. These errors have since been corrected, and this version may be considered the authoritative version of record.